Molecular Pharmacology Fast Forward. Published on May 3, 2018 as DOI: 10.1124/mol.117.111070
This article has not been copyedited and formatted. The final version may differ from this version.

MOL#111070

Ligand-Specific Signaling Profiles and Resensitization Mechanisms of the Neuromedin U2 Receptor

Khaled Alhosaini, Omar Bahattab, Heider Qassam, R.A. John Challiss, and Gary B. Willars

Department of Molecular and Cell Biology, University of Leicester, Leicester, United Kingdom

Molecular Pharmacology Fast Forward. Published on May 3, 2018 as DOI: 10.1124/mol.117.111070
This article has not been copyedited and formatted. The final version may differ from this version.

Running title: Ligand specificity at NMU2

Address correspondence to: Dr. Gary B. Willars, Department of Molecular and Cell Biology, Henry Wellcome Building, University of Leicester, Lancaster Road, Leicester, LE1 7RH, UK.

Tel.: +44 116 2297147

Fax: +44 116 229 7123

E-mail gbw2@leicester.ac.uk

Number of text pages: 36

Number of tables: 1

Number of figures: 12

Number of references: 58

Number of words:

Abstract, 232

Introduction, 664

Discussion, 1500

ABBREVIATIONS: $[Ca^{2+}]_i$, intracellular Ca^{2+} concentration; Cy3B-pNmU-8, fluorescently-labeled porcine neuromedin U-8; ECE-1, endothelin-converting enzyme-1; EGFP, enhanced green fluorescent protein; ERK, extracellular signal-regulated kinase; fluo-4-AM, fluo-4 acetoxymethylester; GPCR, G protein-coupled receptor; HEK, human embryonic kidney; HEK-NMU2, HEK293 cells stably expressing human neuromedin U receptor 2; hNmS-33, human neuromedin S; hNmU-25, human neuromedin U; KHB, Krebs-HEPES buffer; NmS, neuromedin S; NmU, neuromedin U; NMU1, neuromedin U receptor 1; NMU2, neuromedin U receptor 2; p38, p38 mitogen-activated protein kinase; siRNA, short-interfering RNA.

Molecular Pharmacology Fast Forward. Published on May 3, 2018 as DOI: 10.1124/mol.117.111070
This article has not been copyedited and formatted. The final version may differ from this version.

ABSTRACT

The structurally related, but distinct neuropeptides, neuromedin U (NmU) and neuromedin S (NmS) are ligands of two G protein-coupled NmU receptors (NMU1, NMU2). Hypothalamic NMU2 regulates feeding behavior and energy expenditure and has therapeutic potential as an anti-obesity target, making an understanding of its signaling and regulation of particular interest. NMU2 binds both NmU and NmS with high affinity, resulting in receptor-ligand co-internalization. We have investigated whether receptor trafficking events post-internalization are 'biased' by the ligand bound and can therefore influence signaling function. Using recombinant cell-lines expressing human NMU2, we demonstrate that acute Ca^{2+} signaling responses to NmU or NmS are indistinguishable and that restoration of responsiveness (resensitization) requires receptor internalization and endosomal acidification. The rate of NMU2 resensitization is faster following NmU compared to NmS exposure, but is similar if endothelin-converting enzyme-1 activity is inhibited or knocked-down. Although acute activation of extracellular signal-regulated kinase (ERK) is also similar, activation by NMU2 is longer-lasting if NmS is the ligand. Furthermore, when cells were briefly challenged before removal of free, but not receptor-bound ligand, activation of ERK and p38 mitogen-activated protein kinase by NmS is more sustained, but only NmU responses are potentiated and extended by ECE-1 inhibition. These data indicate that differential intracellular ligand processing produces different signaling and receptor resensitization profiles and add to the findings of other studies demonstrating that intracellular ligand processing can shape receptor behavior and signal transduction.

Molecular Pharmacology Fast Forward. Published on May 3, 2018 as DOI: 10.1124/mol.117.111070
This article has not been copyedited and formatted. The final version may differ from this version.

Introduction

The neuropeptide, neuromedin U (NmU) is widely distributed both in the central nervous system and in the periphery, particularly the gastrointestinal tract. NmU has been shown to be involved in an array of physiological and pathological events, including, smooth muscle contraction (Brighton et al., 2008; Mitchell et al., 2009b; Prendergast et al., 2006), thermogenesis, locomotor activity, satiety (Hanada et al., 2004; Howard et al., 2000), glucose homeostasis (Kaczmarek et al., 2006; Peier et al., 2011), inflammatory processes (Johnson et al., 2004; Moriyama et al., 2006b; Moriyama et al., 2006a; Moriyama et al., 2005) and cancer (Alevizos et al., 2001; Harten et al., 2011; Rani et al., 2014; Shetzline et al., 2004). NmU mediates these actions via two G protein-coupled receptors (GPCRs), NMU1 and NMU2, which are family A GPCRs that share ~50% homology (Hosoya et al., 2000; Howard et al., 2000; Kojima et al., 2000; Raddatz et al., 2000; Shan et al., 2000; Szekeres et al., 2000). These receptors show distinct patterns of distribution, with NMU1 having a predominantly peripheral distribution and NMU2 being found primarily in the central nervous system, particularly in the hypothalamus, where it plays a key role in the control of appetite, energy expenditure and the circadian rhythm (Mitchell et al., 2009a). Both NMU1 and NMU2 preferentially couple to $G\alpha_{q/11}$ to regulate the activity of phospholipase C, with a number of reports also highlighting $G\alpha_{i/o}$ coupling to inhibit adenylyl cyclase activity (Aiyar et al., 2004; Brighton et al., 2004).

More recently, neuromedin S (NmS) has been identified as an alternate endogenous ligand for both NMU1 and NMU2 (Miyazato et al., 2008; Mori et al., 2005) NmS shows a more restricted distribution than NmU, being present primarily in the central nervous system, particularly the suprachiasmatic nucleus of the hypothalamus, where it regulates the circadian rhythm of locomotor activity (Mori et al., 2005). NmU and NmS have generated drug discovery interest, particularly given their abilities to regulate feeding behavior and energy homeostasis. Although peripherally located receptors are able to contribute significantly to these effects (Malendowicz et al., 2012; Nakahara et al., 2010) most attention has been focused on central, hypothalamic actions, where NMU2 is thought to be critical. Thus, intracerebroventricular administration of either NmU or NmS reduces feeding behavior in rodents, potentially through regulating hypothalamic corticotropin-releasing hormone release. Interestingly, central administration of NmS mediates a number of these effects for longer

Molecular Pharmacology Fast Forward. Published on May 3, 2018 as DOI: 10.1124/mol.117.111070
This article has not been copyedited and formatted. The final version may differ from this version.

than NmU, including reduced feeding behavior and increases in plasma oxytocin levels (Mori et al., 2005). It has been suggested that a potential explanation for such differences might be a greater resistance to proteolytic degradation of NmS compared to NmU. Indeed, aside from the absolutely conserved *C*-terminal heptapeptide in human versions of the two peptides (*cf.* octapeptide in rat peptides), there is relatively low sequence homology in the remaining *N*-terminal portions of the peptides, providing ample opportunity for differential interactions and/or degradation by proteases. However, given that there are now many examples of different ligands causing distinct (*biased*) signaling events at the same GPCR (Stott et al., 2016; Thompson et al., 2015) such alternate possibilities should be considered in accounting for the variation in the responses to centrally administered NmU and NmS.

Both NmU and NmS bind to their receptors with high affinity (Mitchell et al., 2009b), with an indication that NmS might bind to NMU2 with marginally higher affinity than NmU (Mori et al., 2005). Despite this, in assays of cell signaling, particularly the elevation of intracellular Ca^{2+} concentration ($[Ca^{2+}]_i$), NmU and NmS show equivalent potency and intrinsic activity at both NMU1 and NMU2 (Mitchell et al., 2009b). Assessment of transient Ca^{2+} signals might however not reflect the full extent of the signaling pathways activated by these receptors, including any additional complexities of receptor regulation, and signaling bias displayed by the different endogenous ligands. In the present study we have explored signaling and receptor regulation in response to NmU and NmS at NMU2 and demonstrate key differences between these two endogenous ligands that are of potential physiological and therapeutic importance.

Molecular Pharmacology Fast Forward. Published on May 3, 2018 as DOI: 10.1124/mol.117.111070
This article has not been copyedited and formatted. The final version may differ from this version.

Materials and Methods

Materials. Minimum essential medium with Earle's salts, fetal bovine serum, Dulbecco's phosphate-buffered saline without calcium and magnesium, penicillin (10,000 unit/mL) and streptomycin (10,000 µg/mL) were from Fisher Scientific (Loughborough, UK). Pluronic acid F-127 was from Molecular Probes (Eugene, USA). Bovine serum albumin, poly-D-lysine, fluo-4-acetoxymethylester (fluo-4-AM), cycloheximide, monensin, dynasore, SM-19712 (4-chloro-N-[[(4-cyano-3-methyl-1-phenyl-1H-pyrazol-5-yl)amino]carbonyl]benzenesulfon amide sodium salt hydrate) and carbachol were from Sigma-Aldrich (Poole, UK). Human neuromedin U (hNmU-25) and human neuromedin S (hNmS-33) were purchased from Bachem (St. Helens, UK). Fluorescently-labelled porcine NmU-8 (Cy3B-pNmU-8) was a kind gift from GlaxoSmithKline. Polyvinylidene fluoride membrane was purchased from Millipore (UK) Ltd. (Watford, UK). Pre-stained protein ladders were from Fermentas (Leon-Rot, Germany). Greiner ELISA 96-well plates (8 well/strip) were from Scientific Laboratory Supplies Ltd. (Nottingham, UK). Rabbit monoclonal phospho-p44/42 mitogen-activated protein (MAP) kinases (MAPK, ERK1/2, Thr202/Tyr204) antibody, rabbit polyclonal p42 mitogen-activated protein kinase (MAPK) (extracellular signal-regulated kinase; ERK2) antibody, rabbit monoclonal S6 ribosomal protein antibody, rabbit polyclonal phospho-p38 MAPK (Thr180/Tyr182) and horseradish peroxidase-linked anti-rabbit IgG secondary antibody were from New England Biolabs (UK) Ltd. (Hitchin, UK). Rabbit IgG polyclonal anti- endothelin-converting enzyme-1 (ECE-1) antibody (GTX113676) was from GeneTex (CA, USA). OptiLight chemiluminescent substrate solution was purchased from Cheshire Sciences (UK) Ltd. (Chester, UK). The pEGFP-N1 plasmid, containing the coding sequence for enhanced green fluorescent protein (EGFP), was purchased from Clontech (Oxford, UK). Lipofectamine RNAmaxi for transfection of short interfering RNA (siRNA) was purchased from Invitrogen (Paisley, U.K.). ON-TARGET plus SMART pool consisting of four distinct siRNA duplexes of siRNA targeted to human ECE-1 mRNA and the scrambled siRNA were from ThermoFisher Scientific (New Jersey, U.S.A.) and Invitrogen (Paisley, U.K.), respectively.

Cell Culture. HEK293 cells with stable expression of human NMU2 (HEK-NMU2) have been described and characterized previously (Brighton et al., 2004). Cells were cultured in minimal essential medium with Earle's salts, supplemented with fetal bovine serum (10%

Molecular Pharmacology Fast Forward. Published on May 3, 2018 as DOI: 10.1124/mol.117.111070
This article has not been copyedited and formatted. The final version may differ from this version.

v/v), penicillin and streptomycin (1% *v/v* of purchased stocks) and grown in 75 cm^2 flasks maintained in a humidified environment of 95% air and 5% CO_2 at 37°C. Cultures were passaged every 3-5 days, or as required for experiments.

Measurement of Changes in Intracellular Ca^{2+} Concentration ($[Ca^{2+}]_i$). Changes in $[Ca^{2+}]_i$ were monitored in either single cells by confocal microscopy, or in cell populations using a NOVOstar plate-reader (BMG Labtech, Ortenberg, Germany). For imaging experiments cells were cultured on 25 mm diameter coverslips for 24-48 h to approximately 60% confluence and then loaded with the fluorescent Ca^{2+} indicator fluo-4 by incubation for 45 min at 37°C in Krebs-HEPES buffer (KHB: NaCl, 118 mM; KCl, 4.7 mM; HEPES, 10 mM; glucose, 11.7 mM; $MgSO_4$, 1.2 mM; $NaHCO_3$, 4.2 mM; KH_2PO_4, 1.2 mM; $CaCl_2$, 1.3 mM; bovine serum albumin 0.1% *w/v*, pH 7.4) containing fluo-4-AM (2 μM) and pluronic acid F-127 (0.036%, *w/v*). Following a brief wash, the coverslips were mounted to form the base of a perfusion chamber and KHB (450 μL) added. Images were taken using an Olympus inverted microscope with a 60x oil immersion lens and a PerkinElmer Ultra*VIEW* confocal imaging system (PerkinElmer LAS (UK) Ltd, Beaconsfield, UK) using a laser excitation wavelength of 488 nm and emitted light collected at wavelengths >510 nm. Images were collected at a rate of approximately 1 frame s^{-1} with an exposure multiplier of 1, exposure times of ~200 ms and either 1 x 1 or 2 x 2 binning. Minimum and maximum levels of the grey scales of images were adjusted between 0 and approximately 1000 against a full scale of 4096. Temperature was maintained at 37°C by a Peltier unit (Harvard Applications Inc., Kent, UK). Basal images were taken at least 30 s before bath addition agonist. The change in fluorescence was recorded within a cytosolic region of interest using Ultra*VIEW* 4.0 software and analyzed as an index of $[Ca^{2+}]_i$ relative to the basal levels. In experiments where repetitive agonist additions were made, washes between additions were performed by perfusion of the cells with KHB (5 mL/min). During these experiments, agonist additions were made after ensuring that the focus was stable and no further adjustments made. Recording in the interval between agonist additions was stopped to avoid photobleaching. In re-sensitization experiments where the recovery period was >45 min, initial stimulation was performed on unloaded cells that were subsequently loaded with fluo-4 during the last 45 min of the experiment prior to measurement of $[Ca^{2+}]_i$. Ca^{2+} signaling experiments were performed at 37°C.

Molecular Pharmacology Fast Forward. Published on May 3, 2018 as DOI: 10.1124/mol.117.111070
This article has not been copyedited and formatted. The final version may differ from this version.

For cell population studies, cells were plated in poly-D-lysine-coated 8-well strips of a 96-well plate format for 24 h. On the day of experiments, growth medium was aspirated and the cells were washed twice with KHB and loaded with fluo-4-AM as described above. Cells were then washed once with KHB and incubated with 100 µL KHB at 37°C for 5 min. Using a NOVOstar plate-reader, changes in fluorescence were then determined as an index of changes in $[Ca^{2+}]_i$. Automated additions were of 20 µL made at a speed of 230 µL/s. In protocols in which Ca^{2+} signaling by NMU2 was used to examine desensitization and re-sensitization, the initial challenge was performed manually using the same volume as the automated additions. In these experiments, the 45 min loading of fluo-4-AM and 5 min post-loading incubation were always in the 50 min immediately prior to the measurement of Ca^{2+} signaling. Where required, the equation $[Ca^{2+}]_i = K_d*(F-F_{min})/(F_{max}-F)$ was used in order to convert measurements of fluo-4 fluorescence (F) in populations of cells into $[Ca^{2+}]_i$, where the K_d of fluo-4-AM was taken as 350 nM (Yamasaki-Mann et al., 2009). Maximal fluorescence (F_{max}) was determined by the addition of ionomycin (2 µM) and 4 mM Ca^{2+} to selected wells for up to 10 min. Minimal fluorescence (F_{min}) was then obtained by replacing the buffer with 150 µL of Ca^{2+}-free buffer containing 2 mM EGTA for up to 10 min.

Chemical Treatments in Resensitization Experiments. All of the chemical interventions in the re-sensitization experiments were begun 30-60 min (stated in *Results*) prior to the first challenge with agonist (desensitizing challenge) and continued throughout all subsequent experimental steps, unless otherwise stated.

Imaging Cy3B-pNmU-8 Binding to HEK-NMU2. Cy3B-pNmU-8 binding to HEK-NMU2 was visualized using confocal microscopy with an excitation wavelength of 568 nm. Briefly, cells were cultured on poly-D-lysine-coated 25 mm diameter glass coverslips for 24-48 h. Cells were then washed with KHB, the coverslips mounted to form the base of a perfusion chamber and KHB (450 µL) added. Direct bath addition of Cy3B-pNmU-8 (10 nM final concentration) was performed and images taken using an Olympus inverted microscope with a 60x oil immersion lens and a PerkinElmer Ultra*VIEW* confocal imaging system. Cells were excited using a Kr/Ar laser at a wavelength of 568 nm and emission was collected at approximately 570 nm using a red-green-blue filter. Temperature was maintained at 37°C by a Peltier unit. For experiments where long washing periods were required or a different pH buffer used, cells were perfused at 5mL/min using the appropriate buffer.

Receptor and Ligand Internalization. The cDNA encoding human NMU2 was inserted into the pEGFP-N1 plasmid in order to allow expression of NMU2 with a *C*-terminal EGFP tag. HEK293 cells were transfected and a stable cell-line selected. NMU2-EGFP-expressing cells were cultured on glass coverslips for confocal microscopy imaging of NMU2-EGFP using 488 nm excitation (see above). For dual confocal imaging of NMU2-EGFP and Cy3B-pNmU-8, cells were imaged alternately with 488 nm and 568 nm excitation as described above. Internalization of NMU2-EGFP was quantified using the open source, image processing program, ImageJ. For individual cells, fluorescence intensity was measured at a region of the plasma membrane and within the cytosolic compartment. After subtraction of background fluorescence calculated from regions of the images lacking cells, a measure of internalization was derived using the following equation: internalization = $1-(Fm_t/Fc_t)/(Fm_b/Fc_b)$, where Fm is the membrane fluorescence, Fc is the cytoplasmic fluorescence and *t* is time (of measurement); Fm_b and Fc_b represent these parameters under basal (*b*) conditions at the start of the experiment (0 min).

Knockdown of ECE-1 Expression. For ECE-1 knockdown, cells were plated into poly-D-lysine coated 24-well plates and left to attach for 5-6 h (50-60% confluence). The medium was replaced with Opti-MEM (without serum; 500 μL /well). Lipofectamine RNAmaxi reagent was diluted in Opti-MEM (3:50 *v:v*) and another equal volume of Opti-MEM containing an appropriate amount of either siRNA against ECE-1 or a scrambled version (10 pmol/well) was prepared. The diluted siRNA was then added into the diluted reagent (1:1 *v:v*). After 20 min incubation at room temperature, the siRNA complex was added into each well (100 μL). After approximately 16 h incubation, the medium was replaced with fresh complete medium. The cells were used 48 h after transfection. Knockdown of ECE-1 was confirmed by immunoblotting with an anti-ECE-1 antibody (1:1000), using immunoblotting with an antibody against total ERK (1:1000) as a loading control using the protocol described below.

Determining ERK and p38 MAPK Activity. The activation of ERK and p38 MAPK were determined by immunoblotting of phospho-ERK (pERK) and phospho-p38 MAPK (pp38), respectively. Cell monolayers on poly-D-lysine-coated 24-well plates were serum-starved overnight and then washed and equilibrated with KHB at 37°C. An appropriate concentration of agonist was then added and cells incubated for the indicated times. In cases where SM-

Molecular Pharmacology Fast Forward. Published on May 3, 2018 as DOI: 10.1124/mol.117.111070
This article has not been copyedited and formatted. The final version may differ from this version.

19712 was used, this was added 30 min prior to agonist challenge unless stated otherwise and left in place through subsequent manipulations. Incubations were terminated by aspiration and addition of ice-cold solubilization/sample buffer (Tris-base, 125 mM; Na_3VO_4 1 mM; SDS, 10% (*w/v*); glycerol, 50% *v/v*; bromophenol blue, 0.01% *w/v*; dithiothreitol, 250 mM, adjusted to pH 6.8). Cell lysates were sonicated with a Sonifier ultrasonic cell disruptor (Branson, CT, USA) for 2 s at 10% of maximal power and then centrifuged (12,000 x*g*; 10 min; 4°C). Supernatants were either used immediately or stored at -80°C until use.

Proteins were separated by SDS-PAGE using a 10% resolving gel and transferred onto polyvinylidene fluoride membranes. Following blocking of the membrane for 1 h at room temperature in Tween-20 buffer (TBST: Tris-base, 50 mM, pH 7.5; NaCl, 150 mM; Tween-20, 0.05% *v/v*) containing 5% bovine serum albumin, membranes were probed overnight at 4°C using either rabbit monoclonal phospho-p44/42 MAPK (phospho-ERK1/2) antibody (1:2000), phospho-p38 (1:1000) or rabbit monoclonal S6 ribosomal protein antibody (1:20000). Following washing, membranes were incubated in TBST with 5% (*w/v*) fat-free milk containing goat anti-rabbit IgG, horseradish peroxidase-linked secondary antibody (1:3000) for 60 min at RT. Detection was performed by applying OptiLight chemiluminescent reagent. Using ribosomal S6 band intensities, loading was assessed to be equivalent before analysis of the band intensities of the phospho-proteins. To allow direct comparison of band intensities, all samples for each experimental replicate in which the effects of hNmU-25 and hNmS-33 in the presence and absence of the ECE-1 inhibitor (SM-19712) were to be compared were run together and ultimately exposed on the same piece of film.

Data Analysis. Data were analyzed using Prism software (v7.0; GraphPad Software Inc., San Diego, USA) and expressed as means ± s.e.m. unless otherwise stated. Where representative data are shown, these are of at least three independent experiments. To construct concentration-response curves for agonist-mediated changes in $[Ca^{2+}]_i$, the maximal changes in fluorescence were subtracted from the basal values. Concentration-response curves were fit for each experiment using a 4 parameter logistical equation to allow determination of individual maximal values (E_{max}) and pEC_{50} values ($-\log_{10}$ M EC_{50}) for any subsequent descriptive or comparative statistical analyses: curves of the mean data of all experiments are displayed in the figures. For measuring the recovery of either Ca^{2+} concentration-response curves, or maximal Ca^{2+} responses, changes in fluorescence were expressed as a percentage

Molecular Pharmacology Fast Forward. Published on May 3, 2018 as DOI: 10.1124/mol.117.111070
This article has not been copyedited and formatted. The final version may differ from this version.

of the maximum response in cells pre-exposed to buffer only (i.e. no initial agonist challenge). All statistical analyses were performed on the raw data before normalization. In recovery experiments, for each recovery time-point, a control-response was also measured. Comparative statistics were performed using one-way ANOVA followed by an appropriate range test with $P<0.05$ considered significant.

Molecular Pharmacology Fast Forward. Published on May 3, 2018 as DOI: 10.1124/mol.117.111070
This article has not been copyedited and formatted. The final version may differ from this version.

Results

Single-Cell Ca^{2+} Responses to hNmU-25. Confocal fluorescence imaging of adherent, fluo-4-loaded HEK-NMU2 cells demonstrated a rapid, transient elevation of $[Ca^{2+}]_i$ following addition of hNmU-25 (30 nM) (Fig. 1A). To examine NMU2 desensitization, cells were perfused for 5 min with KHB following an initial 60 s challenge with hNmU-25. Re-application of hNmU-25 failed to evoke any increase in $[Ca^{2+}]_i$ (Fig. 1A), consistent with our previous findings (Brighton et al., 2004). In contrast, employing a similar protocol, we could demonstrate a partial desensitization (40 ± 2% of initial response) of an endogenous M_3 muscarinic acetylcholine receptor when measuring $[Ca^{2+}]_i$ responses (Fig. 1B).

Developing a Protocol to Remove Completely Cell-Bound Ligand. Our previous studies demonstrated that NmU binding to NMU receptors is essentially irreversible (Brighton et al., 2004). In order to examine whether the observed functional desensitization of NMU2 Ca^{2+} signaling was altered by ligand removal, we developed a protocol to dissociate ligand from cell-surface receptors, without compromising Ca^{2+} signaling or cell viability (see below). Using confocal imaging of Cy3B-pNmU-8, we have shown that a rapid acid wash procedure removes cell-bound NmU without negatively impacting receptor-mediated Ca^{2+} signaling or cell viability. Thus, addition of Cy3B-pNmU-8 to NMU2 resulted in intense membrane-localized fluorescence that was unaffected by subsequent perfusion with standard KHB (pH 7.4) (Fig. 2Ai and Aii). Perfusion for 15-25 s with acidic KHB solutions at pH 4.0 (Fig. 2Aiii), 3.5 (Fig. 2Aiv) or 3.0 (Fig. 2Av) failed to displace membrane fluorescence, but exposure to pH 2.0 completely removed membrane fluorescence (Fig. 2Avi). Fluorescence was not restored by a 5 min wash with standard KHB, indicating ligand removal rather than quenching of fluorescence (Fig. 2Bi-iii). Moreover, re-application of Cy3B-pNmU-8 to these cells restored membrane fluorescence (Fig. 2Biv) indicating that NMU2 was able to rebind ligand.

To determine whether the brief acid wash influenced receptor-mediated Ca^{2+} signaling, HEK-NMU2 were first washed briefly (≤25 s) with KHB at either pH 2.0 or pH 7.4, followed by either a 5 or 120 min period in KHB, pH 7.4, before determining Ca^{2+} responses. The brief wash with acidified buffer did not affect hNmU-25-mediated Ca^{2+} responses in ligand-naïve cells (pEC_{50} values: 9.17 ± 0.02 and 9.18 ± 0.10 with KHB, pH 2.0 wash and 5 or 120 min

Molecular Pharmacology Fast Forward. Published on May 3, 2018 as DOI: 10.1124/mol.117.111070
This article has not been copyedited and formatted. The final version may differ from this version.

recovery, respectively; 9.43 ± 0.08 and 9.16 ± 0.11 with pH 7.4 wash and 5 or 120 min recovery, respectively: Fig. 3A, B). Furthermore, cell viability, as assessed by confocal imaging of trypan blue exclusion, was unaffected by the wash with acidified KHB (cell viability 89 ± 5% at 30 min following acid wash compared to 90 ± 7% following wash with KHB, pH 7.4). Extending the wash with KHB, pH 2.0 to 45-55 s did, however, have a marked detrimental effect on cell viability (34 ± 5%).

Functional Desensitization of NMU2. Having established a wash procedure that removes surface-bound ligand, but retains receptor-mediated Ca^{2+} signaling and cell viability, this protocol was next used to explore NMU2 desensitization in the absence of ligand bound to cell-surface receptors. When fluo-4-loaded HEK-NMU2 cells were challenged with hNmU-25 (30 nM, 60 s), followed by a brief wash with acidic buffer (KHB, pH 2.0; ≤25 s) and re-perfusion with normal buffer (KHB, pH 7.4; 5 min), re-application of hNmU-25 (30 nM) now resulted in a Ca^{2+} response that was 56 ± 8% of the initial agonist-stimulated response (n=3, Fig. 3C). In the same series of experiments using carbachol instead of hNmU-25, the Ca^{2+} response to the re-challenge with carbachol was 39 ± 8% of the initial response (n=3; Fig. 3D), similar to the extent of M_3 muscarinic acetylcholine receptor 'desensitization' observed previously (Fig. 1B).

Resensitization in the Absence or Continuing Presence of Extracellular Ligand. To assess the impact of the duration of ligand exposure on the subsequent desensitization, HEK-NMU2 cells were exposed to a maximally-effective concentration of hNmU-25 (30 nM) for 1, 3, 5 or 30 min. Ligand was then removed with a brief KHB, pH 2.0 wash and subsequent washing with KHB, pH 7.4; cells were then allowed to recover for 5 min before re-challenge with the same concentration of hNmU-25 (Fig. 4A). A rapid, progressive reduction in the Ca^{2+} response to re-challenge was observed as the duration of the initial challenge was increased from 1 to 5 min (Fig. 4B), while increasing the duration of the initial challenge from 5 to 30 min did not further reduce the response to hNmU-25 re-challenge (Fig. 4B, C).

To determine (i) the time-course of receptor resensitization and (ii) the effect of ongoing ligand binding to NMU2, cells were challenged with a maximal concentration of hNmU-25 (30 nM) for 5 min and then washed with either KHB, pH 2.0 or KHB, pH 7.4. Following recovery periods of 5 to 360 min in standard KHB, Ca^{2+} responses on re-challenge with

Molecular Pharmacology Fast Forward. Published on May 3, 2018 as DOI: 10.1124/mol.117.111070
This article has not been copyedited and formatted. The final version may differ from this version.

different concentrations of hNmU-25 (0.1-100 nM) were assessed. In the absence of the brief acid wash to unbind ligand from receptor, functional recovery of the full intrinsic activity (E_{max}) and potency (EC_{50}) of hNmU-25 required ~300 min (Fig. 5A). In contrast, when the acid wash procedure was applied to cells, full recovery of agonist-stimulated Ca^{2+} signaling occurred within approx. 120 min (Fig. 5B). These data provide strong evidence that the presence of ligand bound to receptors prolonged the time required for resensitization of NMU2-mediated Ca^{2+} signaling.

hNmS-33 and hNmU-25 are Equipotent, Full Agonists at NMU2, but Differ in their Effects on Receptor Desensitization/Resensitization. NmS has been identified as a second endogenous ligand for NMU receptors, in particular for those expressed centrally (Miyazato et al., 2008; Mori et al., 2005). NmS and NmU bind with similar affinity to NMU receptors and, consistent with other studies, we have shown that hNmS-33 mediates Ca^{2+} signaling at NMU2 with equivalent maximal responses and potency to hNmU-25 (pEC_{50} (-log M) values: hNmU-25, 9.18 ± 0.05; hNmS-33, 9.30 ± 0.10; n=4).

Here we compared the rates of re-sensitization of NMU2-mediated Ca^{2+} signaling following a 5 min challenge with either hNmU-25 (30 nM) or hNmS-33 (30 nM) under conditions where free ligand, but not receptor-bound ligand was removed by washing with KHB, pH 7.4. Challenge of HEK-NMU2 with either ligand, followed by washing and a 5 min recovery period, resulted in equivalent and marked reductions in Ca^{2+} signaling (Fig. 6A, B). The time-courses of recovery following the desensitization protocol were also determined for each ligand. Under these conditions, NMU2-mediated Ca^{2+} signaling was fully restored following a 360 min recovery period after initial challenge with hNmU-25, however, only approximately 50% of the Ca^{2+} response was recovered in this time-period when hNmS-33 was applied as the desensitizing stimulus (Fig. 6C).

Co-Internalization of Ligand and Receptor. Ligands that bind with high-affinity are likely to be co-internalized with the receptor (Oakley et al., 2001). Here we show that this is true for Cy3B-pNmU-8 that co-internalizes with NMU2 in a HEK cell-line stably expressing *C*-terminally EGFP-tagged NMU2 (NMU2-EGFP) (Fig. 7A). Time-courses of NMU2-EGFP were also quantified following application of hNmU-25 or hNmS-33, with the profiles of

Molecular Pharmacology Fast Forward. Published on May 3, 2018 as DOI: 10.1124/mol.117.111070
This article has not been copyedited and formatted. The final version may differ from this version.

NMU2-EGFP internalization being essentially indistinguishable in extent and profile for the two ligands (Fig. 7B, C)

Mechanistic Insights into the Resensitization of NMU2. A mechanistic understanding of the NMU2 resensitization process requires knowledge of how the ligand-receptor complex is endocytosed and processed towards recycling. The dynamin GTPase inhibitor, dynasore (80 μM) (Macia et al., 2006), markedly reduced resensitization of NMU2 signaling following challenge with either hNmU-25 (Fig. 8A) or hNmS-33 (Fig. 8B). Inhibition of endosomal acidification with either monensin (50 μM) (Fig. 8C, D) or bafilomycin A (200 nM; data not shown) also significantly reduced resensitization following challenge with either ligand. In contrast, a concentration of cycloheximide (17.5 μM) that markedly reduced protein synthesis (>80% reduction based on incorporation of [^{35}S]-methionine into HEK cell total protein) had no significant impact on resensitization following challenge with either ligand (Fig. 8D, E). None of these pre-treatments (dynasore, monensin, or cycloheximide) affected Ca^{2+} responses of naïve HEK-NMU2 cells to hNmU-25 or hNmS-33 (data not shown). Taken together, these data indicate that dynamin-dependent NMU2 internalization and endosomal acidification, but not *de novo* synthesis of NMU2, are required for resensitization of NMU2-mediated Ca^{2+} signaling irrespective of the agonist mediating the initial desensitization.

Role of Ligand Processing in the Resensitization of NMU2. Given that bound hNmU-25 and hNmS-33 will internalize with NMU2, we next considered if ligand processing might occur during NMU2 recycling and whether differences in the processing of hNmU-25 and hNmS-33 might account for differing rates of resensitization. Previous studies have shown that endothelin-converting enzyme 1 (ECE-1) plays a role in the endosomal processing of a number of peptide ligands (Law et al., 2012; Padilla et al., 2007; Roosterman et al., 2007; Roosterman et al., 2008). Here we explored the potential role of ECE-1 in the processing of the endogenous NMU2 ligands using the ECE-1 inhibitor, SM-19712 (Umekawa et al., 2000). SM-19712 (10 μM; 30 min pre-treatment) significantly reduced the rate of resensitization of the Ca^{2+} response to hNmU-25 (Fig. 9A), but was without effect on the recovery of Ca^{2+} signaling following challenge with hNmS-33 (Fig. 9B) in HEK-NMU2 cells. SM-19712 also had no detectable effect on the much more rapid recovery of Ca^{2+} responses to carbachol (300 μM) following an initial activation of the endogenous M_3 muscarinic acetylcholine receptors with this ligand (Fig. 9C). SM-19712 (10 or 100 μM) was without effect on Ca^{2+} responses to

either hNmU-25 or hNmS-33 in ligand-naïve cells (data not shown). The neutral endopeptidase inhibitor, thiorphan (10 μM), did not significantly alter re-sensitization time-courses to either hNmU-25 or hNmS-33 (data not shown).

The ability of SM-19712 selectively to reduce the recovery of Ca^{2+} responses to re-challenge with hNmU-25 might be explained by: (1) the protection of extracellular peptide from degradation (thereby potentially enhancing the extent of the initial stimulation and potential desensitization) and/or (2) the protection of intracellular peptide from degradation (thereby potentially reducing the rate of receptor recycling and subsequent resensitization). To assess these possibilities, experiments were conducted in which SM-19712 was added only after the initial stimulation and removal of free hNmU-25. When SM-19712 was added only to be present after removal of the initial challenge with hNmU-25, the extent of inhibition of re-sensitization was comparable to that observed when the inhibitor was added 30 min before the desensitizing exposure to ligand (Fig. 9D), suggesting that protection from post-internalization processing contributes to the action of this inhibitor.

Transfection of cells with siRNA against ECE-1 resulted in a significant reduction in expression (to 31 ± 4% of control levels; Fig. 10A). This knockdown of expression was associated with a marked inhibition of NMU2 resensitization following pre-challenge with hNmU-25 (Fig. 10B), but was without effect on the rather slower re-sensitization seen following pre-challenge with hNmS-33 (Fig. 10C).

Ligand-Dependent Regulation of ERK and p38 MAPK Activity in HEK-NMU2. Challenge of HEK-NMU2 cells with either hNmU-25 or hNmS-33 (30 nM) resulted in time-dependent increases in phospho-ERK that remained elevated for at least 3 h in the continued presence of ligand (Fig. 11A, B). It was noteworthy that the phospho-ERK response to hNmS-33 was better sustained (Fig. 11B) compared to the hNmU-25 response (Fig. 11A). Agonist-stimulated increases in phospho-ERK were concentration-dependent (pEC_{50} (-log M) values 8.54 ± 0.07 and 8.83 ± 0.08 (n=3) at 5 min for hNmU-25 and hNmS-33, respectively). Under these experimental conditions, where ligand was not removed, pre-addition of the ECE-1 inhibitor, SM-19712 (10 μM), had no effect on either the magnitude or temporal profile of ERK activation stimulated by either ligand (Fig. 11A, B).

Molecular Pharmacology Fast Forward. Published on May 3, 2018 as DOI: 10.1124/mol.117.111070
This article has not been copyedited and formatted. The final version may differ from this version.

Removal of free hNmS-33 using a buffer wash after 5 min stimulation resulted in a slow decline in the levels of phospho-ERK, but this was still approximately 40% of the initial response 180 min after removal of free, extracellular ligand (Fig. 12B). In contrast, removal of free hNmU-25 using a buffer wash after 5 min stimulation resulted in a faster and greater loss of phospho-ERK, such that at 180 min after removal of free, extracellular ligand, phospho-ERK immunoreactivity had returned to basal levels (Fig. 12A). Pre-addition of SM-19712 had no impact on the time-course of the phospho-ERK response following addition and withdrawal of hNmS-33 (Fig, 12B), however addition of this inhibitor significantly increased and prolonged the phospho-ERK response following addition and wash-removal of hNmU-25 (Fig. 12A).

Using a similar protocol (30 nM ligand for 5 min followed by washing to remove free, extracellular ligand) resulted in a relatively sustained increase in the levels of phospho-p38 MAPK (pp38) over the 175 min following ligand withdrawal with pre-addition of SM-19712 having no effect on this time-course (Fig. 12D). In contrast, pp38 responses to hNmU-25 declined between 25 and 175 min after the 5 min agonist addition (Fig. 12C). Pre-addition of SM-19712 significantly increased and prolonged the pp38 response (Fig. 12C). These data demonstrate that the susceptibility of hNmU-25, but not hNmS-33 to the action of ECE-1 generates different ligand-dependent patterns of ERK/p38 MAPK activation.

Molecular Pharmacology Fast Forward. Published on May 3, 2018 as DOI: 10.1124/mol.117.111070
This article has not been copyedited and formatted. The final version may differ from this version.

Discussion

Our previous study established that NmU binds essentially irreversibly to NMU receptors at the plasma membrane (Brighton et al., 2004). Such persistent agonist occupation prevents assessment of receptor desensitization that is independent of continued ligand binding and the possible sustained depletion of signaling components. Here we used a rapid, acid-wash protocol to remove ligand, either free or bound at the cell-surface, to demonstrate that NMU2 desensitization can occur independently from the continued presence of bound ligand. Indeed, the extent of desensitization is comparable to that of the $G\alpha_{q/11}$-coupled M_3 muscarinic receptor that binds low affinity small molecule ligands that are readily removed by simple wash protocols. The present data highlight the additional role played by the essentially irreversible binding of peptides to NMU2 that occurs under physiological conditions.

The present data also demonstrate that ligand binding to NMU2 considerably lengthens the recovery time of receptor-mediated Ca^{2+} signaling. This slow resensitization is similar to that observed for a number of other peptidergic GPCRs. For example, neurokinin 1 receptor Ca^{2+} responses require ~3 h to recover following challenge with substance P, while the CLR/RAMP1 complex needs 4-6 h for full resensitization of CGRP-mediated Ca^{2+} signaling (Padilla et al., 2007; Schmidlin et al., 2001). The slower recovery of signaling following transient exposure to hNmU-25 was markedly faster than that following an identical exposure to hNmS-33, clearly demonstrating the critical nature of the ligand in determining the rate of re-sensitization. Independent of the ligand used, resensitization required receptor internalization and endosomal acidification, but not *de-novo* protein synthesis, which is entirely consistent with the generally accepted paradigm for GPCR trafficking following agonist activation. Thus, agonist-mediated conformational changes in the receptor result in the recruitment of G protein-coupled receptor kinase (GRK) isoenzymes and subsequent phosphorylation of serine/threonine residues within intracellular regions of the receptor, particularly the *C*-terminal tail and third intracellular loop (Pitcher et al., 1998). Such phosphorylation provides docking sites for β-arrestin, which generates steric hindrance to further G protein coupling, thereby initiating rapid receptor desensitization. Bound β-arrestin provides a scaffold for the internalization machinery, ultimately resulting in the removal of receptors from the cell surface into an endosomal compartment. Endosomal acidification promotes dissociation of any internalized ligand with the subsequent loss of β-arrestin

Molecular Pharmacology Fast Forward. Published on May 3, 2018 as DOI: 10.1124/mol.117.111070
This article has not been copyedited and formatted. The final version may differ from this version.

binding, receptor dephosphorylation and ultimately the recycling of receptors to the plasma membrane for further rounds of signaling (Marchese et al., 2008). The time required to fully resensitize differs among GPCRs, ranging from minutes, as for the β_2-adrenoceptor, to hours for some receptors including the V_2 vasopressin receptor (Moore et al., 2007). Such differences are a consequence of various factors, but include the affinity for β-arrestin binding (Oakley et al., 1999; Pierce et al., 2002). In respect of this, different classes of GPCR have been identified. Type A GPCRs bind β-arrestin-2 more favorably than β-arrestin-1, although with relatively low affinity, resulting in rapid dissociation of the receptor-β-arrestin complex at the cell-surface, or directly after internalization, resulting in fast recycling and resensitization (Moore et al., 2007). In contrast, Type B GPCRs bind with high affinity to either β-arrestin-1 or β-arrestin-2, which internalize together with the receptor to endosomes and dissociate at a slow rate, delaying recycling and resensitization (Moore et al., 2007), which is consistent with the slow re-sensitization of NMU2. Although little is known regarding agonist-mediated phosphorylation of NMU2, the *C*-terminal tail contains fifteen serine and threonine residues, including three pairs of serine residues that are often associated with phosphorylation and arrestin binding (Brighton et al., 2004b).

In this scheme of receptor internalization and recycling, attention rarely focuses on either the potential role or fate of the ligand. This is critical given that the presence of ligand, particularly bound to the receptor, may influence the nature and duration of β-arrestin binding. This, in turn, is of particular importance given the role of β-arrestin in scaffolding signaling complexes for both G protein-dependent (Thomsen et al., 2016) and G protein-independent signaling (DeFea, 2011; Luttrell and Miller, 2013; Shenoy and Lefkowitz, 2011) from within the cell. Given the extremely high affinity binding of some peptide ligands and the extent of acidification that is required to drive dissociation, it is possible that some ligands retain receptor association for some time despite endosomal acidification to pH 4.8-6.0 (Hilal-Dandan et al., 1997; Qi et al., 2005). Although some peptide ligands may recycle to the plasma membrane intact, others are processed within the cell. Indeed, a series of important studies have highlighted a key function of such processing within the cell in defining both receptor re-sensitization and the duration of receptor-mediated signaling (Cottrell et al., 2009; Hasdemir et al., 2012; Padilla et al., 2007; Pelayo et al., 2011; Roosterman et al., 2007; Roosterman et al., 2008). In particular, endothelin converting enzyme 1 (ECE-1) is able to

Molecular Pharmacology Fast Forward. Published on May 3, 2018 as DOI: 10.1124/mol.117.111070
This article has not been copyedited and formatted. The final version may differ from this version.

process a number of internalized peptide ligands to regulate receptor signaling and re-cycling. Although ECE-1 is best known for its ability to convert plasma big endothelin to active endothelin-1, the identification of four isoenzymes with differential sub-cellular distributions is consistent with alternative functions, including the degradation of peptide receptor ligands within the endosomal compartment. Interestingly, the substrate specificity of ECE-1 is pH-dependent (Ahn et al., 1998) and the acidic pH of the endosomal compartment provides ideal conditions for the degradation of substance P, calcitonin gene-related peptide and somatostatin 14 (Poole and Bunnett, 2016). Indeed, the degradation of internalized peptide ligands within the endosomal compartment destabilizes signaling complexes and promotes recycling and resensitization of a number of receptors (Cottrell et al., 2009; Hasdemir et al., 2012; Padilla et al., 2007; Pelayo et al., 2011; Roosterman et al., 2007; Roosterman et al., 2008). More recently, sustained signaling by the neurokinin 1 receptor and calcitonin receptor-like receptor from within endosomes has been shown to be responsible for sustained neuronal activity and the transmission of pain (Jensen et al., 2017; Yarwood et al., 2017). Furthermore, targeting receptor antagonists to this compartment was demonstrated to inhibit endosomal signaling and the sustained neuronal activity highlighting novel and exciting therapeutic opportunities.

The present study demonstrates a role for ECE-1 within the cell in promoting NMU2 recycling leading to resensitization, but this is dependent on the nature of the ligand. Pharmacological inhibition of ECE-1 or knockdown with siRNA both inhibit resensitization following hNmU-25, but not hNmS-33, suggesting that either hNmS-33 is resistant to ECE-1 activity within the cell, or that products of its degradation can continue to reduce receptor recycling. Interestingly, like NMU2, the corticotropin-releasing factor receptor 1 (CRF_1) can be activated by either of the two endogenous ligands urocortin or corticotrophin-releasing factor (CRF). Urocortin not only binds to CRF_1 with higher affinity than CRF, but is also a better substrate for ECE-1, providing an explanation for the sensitivity to ECE-1 inhibition of CRF_1 recycling and resensitization following urocortin, but not CRF (Hasdemir et al., 2012).

The present study identified different temporal profiles of ERK signaling, particularly following ligand removal. In particular, NMU2-mediated activation of ERK was more sustained following hNmS-33 than hNmU-25. This is consistent with a more sustained signaling complex, possibly as a consequence of the resistance of hNmS-33 to ECE-1

Molecular Pharmacology Fast Forward. Published on May 3, 2018 as DOI: 10.1124/mol.117.111070
This article has not been copyedited and formatted. The final version may differ from this version.

proteolytic degradation, and sustained G protein-dependent or -independent signaling. Such signaling may be from internalized receptors as NMU2 is markedly internalized. Although the removal of free extracellular ligand is clearly central to experimental studies of resensitization, this has been less commonly used when examining signaling events following a single exposure to ligand. However, such a paradigm may well reflect more accurately the type of exposure that cells are subject to *in vivo*. Thus, receptor ligands are more often than not released in a pulsatile or phasic manner, following which they are removed by a variety of processes including dilution, extracellular degradation and cellular uptake. Although the physiological consequences of transient versus more sustained signaling have yet to be fully defined, the present study highlights that such considerations are critical in identifying ligand-specific signaling profiles and ultimately, therefore, differences in biological activity and therapeutic potential. With specific reference to ligands of NMU2, there is evidence to support the notion that signaling differences, such as those reported here, may be relevant in more physiological settings. Thus, bolus intracerebroventricular administration of NmU to rats increased the neuronal electrical activity in the PVN between 30 and 60 min, whereas NmS increased activity for at least 120 min (Ida et al., 2005). This is potentially consistent with a more potent and prolonged suppression of food intake by NmS compared to NmU following intracerebroventricular administration to freely-feeding rats (Ida et al., 2005; Miyazato et al., 2008). One suggestion for such differences was that NmS might be more resistant to proteolytic degradation than NmU. Clearly such resistance could maintain effective extracellular concentrations of NmS for longer. However, the present study demonstrates an alternative possibility; that cellular signaling at NMU2 in response to NmS is prolonged compared to that in response to NmU. Furthermore, the data suggest that such a disparity is a consequence of differences in the intracellular processing of the two peptide ligands by intracellular, probably endosomal, ECE-1, or a similar SM-19712-sensitive protease.

Molecular Pharmacology Fast Forward. Published on May 3, 2018 as DOI: 10.1124/mol.117.111070
This article has not been copyedited and formatted. The final version may differ from this version.

Authorship Contributions

Participated in research design: Alhosaini, Challiss, Willars.

Conducted the experiments: Alhosaini, Bahattab, Qassam.

Performed data analysis: Alhosaini, Bahattab, Qassam, Challiss, Willars.

Wrote or contributed to the writing of the manuscript: Alhosaini, Challiss, Willars.

Molecular Pharmacology Fast Forward. Published on May 3, 2018 as DOI: 10.1124/mol.117.111070
This article has not been copyedited and formatted. The final version may differ from this version.

References

Ahn K, Herman SB and Fahnoe DC (1998) Soluble human endothelin-converting enzyme-1: Expression, purification, and demonstration of pronounced pH sensitivity. *Arch Biochem Biophys* **359**(2): 258-268.

Aiyar N, Disa J, Foley JJ, Buckley PT, Wixted WE, Pullen M, Shabon U, Dul E, Szekeres PG, Elshourbagy NA, Sarau HM, Appelbaum E and Bolaky J (2004) Radioligand binding and functional characterization of recombinant human NmU1 and NmU2 receptors stably expressed in clonal human embryonic kidney-293 cells. *Pharmacology* **72**(1): 33-41.

Alevizos I, Mahadevappa M, Zhang X, Ohyama H, Kohno Y, Posner M, Gallagher GT, Varvares M, Cohen D, Kim D, Kent R, Donoff RB, Todd R, Yung CM, Warrington JA and Wong DT (2001) Oral cancer in vivo gene expression profiling assisted by laser capture microdissection and microarray analysis. *Oncogene* **20**(43): 6196-6204.

Brighton PJ, Szekeres PG and Willars GB (2004b) Neuromedin U and its receptors: structure, function, and physiological roles. *Pharmacol Rev* **56**(2): 231-248.

Brighton PJ, Szekeres PG, Wise A and Willars GB (2004) Signaling and ligand binding by recombinant neuromedin U receptors: evidence for dual coupling to Galphaq/11 and Galphai and an irreversible ligand-receptor interaction. *Mol Pharmacol* **66**(6): 1544-1556.

Brighton PJ, Wise A, Dass NB and Willars GB (2008) Paradoxical behavior of neuromedin U in isolated smooth muscle cells and intact tissue. *J Pharmacol Exp Ther* **325**(1): 154-164.

Cottrell GS, Padilla BE, Amadesi S, Poole DP, Murphy JE, Hardt M, Roosterman D, Steinhoff M and Bunnett NW (2009) Endosomal endothelin-converting enzyme-1: a regulator of beta-arrestin-dependent ERK signaling. *J Biol Chem* **284**(33): 22411-22425.

DeFea KA (2011) Beta-arrestins as regulators of signal termination and transduction: how do they determine what to scaffold? *Cell Signal* **23**(4): 621-629.

Hanada R, Teranishi H, Pearson JT, Kurokawa M, Hosoda H, Fukushima N, Fukue Y, Serino R, Fujihara H, Ueta Y, Ikawa M, Okabe M, Murakami N, Shirai M, Yoshimatsu H, Kangawa K and Kojima M (2004) Neuromedin U has a novel anorexigenic effect independent of the leptin signaling pathway. *Nat Med* **10**(10): 1067-1073.

Harten SK, Esteban MA, Shukla D, Ashcroft M and Maxwell PH (2011) Inactivation of the von Hippel-Lindau tumour suppressor gene induces Neuromedin U expression in renal cancer cells. *Mol Cancer* **10**(1): 89.

Hasdemir B, Mahajan S, Bunnett NW, Liao M and Bhargava A (2012) Endothelin-converting enzyme-1 actions determine differential trafficking and signaling of corticotropin-releasing factor receptor 1 at high agonist concentrations. *Mol Endocrinol* **26**(4): 681-695.

Hilal-Dandan R, Villegas S, Gonzalez A and Brunton LL (1997) The quasi-irreversible nature of endothelin binding and G protein-linked signaling in cardiac myocytes. *J Pharmacol Exp Ther* **281**(1): 267-273.

Hosoya M, Moriya T, Kawamata Y, Ohkubo S, Fujii R, Matsui H, Shintani Y, Fukusumi S, Habata Y, Hinuma S, Onda H, Nishimura O and Fujino M (2000) Identification and functional characterization of a novel subtype of neuromedin U receptor. *J Biol Chem* **275**(38): 29528-29532.

Howard AD, Wang R, Pong SS, Mellin TN, Strack A, Guan XM, Zeng Z, Williams DL, Jr., Feighner SD, Nunes CN, Murphy B, Stair JN, Yu H, Jiang Q, Clements MK, Tan CP, McKee KK, Hreniuk DL, McDonald TP, Lynch KR, Evans JF, Austin CP, Caskey CT, Van der Ploeg LH and Liu Q (2000) Identification of receptors for neuromedin U and its role in feeding. *Nature* **406**(6791): 70-74.

Ida T, Mori K, Miyazato M, Egi Y, Abe S, Nakahara K, Nishihara M, Kangawa K and Murakami N (2005) Neuromedin s is a novel anorexigenic hormone. *Endocrinology* **146**(10): 4217-4223.

Jensen DD, Lieu T, Halls ML, Veldhuis NA, Imlach WL, Mai QN, Poole DP, Quach T, Aurelio L, Conner J, Herenbrink CK, Barlow N, Simpson JS, Scanlon MJ, Graham B, McCluskey A, Robinson PJ, Escriou V, Nassini R, Materazzi S, Geppetti P, Hicks GA, Christie MJ, Porter CJH, Canals M and Bunnett NW (2017) Neurokinin 1 receptor signaling in endosomes mediates sustained nociception and is a viable therapeutic target for prolonged pain relief. *Sci Transl Med* **9**(392).

Johnson EN, Appelbaum ER, Carpenter DC, Cox RF, Disa J, Foley JJ, Ghosh SK, Naselsky DP, Pullen MA, Sarau HM, Scheff SR, Steplewski KM, Zaks-Zilberman M and Aiyar N (2004)

Neuromedin U elicits cytokine release in murine Th2-type T cell clone D10.G4.1. *J Immunol* **173**(12): 7230-7238.

Kaczmarek P, Malendowicz LK, Pruszynska-Oszmalek E, Wojciechowicz T, Szczepankiewicz D, Szkudelski T and Nowak KW (2006) Neuromedin U receptor 1 expression in the rat endocrine pancreas and evidence suggesting neuromedin U suppressive effect on insulin secretion from isolated rat pancreatic islets. *Int J Mol Med* **18**(5): 951-955.

Kojima M, Haruno R, Nakazato M, Date Y, Murakami N, Hanada R, Matsuo H and Kangawa K (2000) Purification and identification of neuromedin U as an endogenous ligand for an orphan receptor GPR66 (FM3). *Biochem Biophys Res Commun* **276**(2): 435-438.

Law IK, Murphy JE, Bakirtzi K, Bunnett NW and Pothoulakis C (2012) Neurotensin-induced proinflammatory signaling in human colonocytes is regulated by beta-arrestins and endothelin-converting enzyme-1-dependent endocytosis and resensitization of neurotensin receptor 1. *J Biol Chem* **287**(18): 15066-15075.

Luttrell LM and Miller WE (2013) Arrestins as regulators of kinases and phosphatases. *Prog Mol Biol Transl Sci* **118**: 115-147.

Macia E, Ehrlich M, Massol R, Boucrot E, Brunner C and Kirchhausen T (2006) Dynasore, a cell-permeable inhibitor of dynamin. *Dev Cell* **10**(6): 839-850.

Malendowicz LK, Ziolkowska A and Rucinski M (2012) Neuromedins U and S involvement in the regulation of the hypothalamo-pituitary-adrenal axis. *Frontiers in endocrinology* **3**: 156.

Marchese A, Paing MM, Temple BR and Trejo J (2008) G protein-coupled receptor sorting to endosomes and lysosomes. *Annu Rev Pharmacol Toxicol* **48**: 601-629.

Mitchell JD, Maguire JJ and Davenport AP (2009a) Emerging pharmacology and physiology of neuromedin U and the structurally related peptide neuromedin S. *Br J Pharmacol* **158**(1): 87-103.

Mitchell JD, Maguire JJ, Kuc RE and Davenport AP (2009b) Expression and vasoconstrictor function of anorexigenic peptides neuromedin U-25 and S in the human cardiovascular system. *Cardiovasc Res* **81**(2): 353-361.

Miyazato M, Mori K, Ida T, Kojima M, Murakami N and Kangawa K (2008) Identification and functional analysis of a novel ligand for G protein-coupled receptor, Neuromedin S. *Regul Pept* **145**(1-3): 37-41.

Moore CA, Milano SK and Benovic JL (2007) Regulation of receptor trafficking by GRKs and arrestins. *Annu Rev Physiol* **69**: 451-482.

Mori K, Miyazato M, Ida T, Murakami N, Serino R, Ueta Y, Kojima M and Kangawa K (2005) Identification of neuromedin S and its possible role in the mammalian circadian oscillator system. *Embo J* **24**(2): 325-335.

Moriyama M, Fukuyama S, Inoue H, Matsumoto T, Sato T, Tanaka K, Kinjyo I, Kano T, Yoshimura A and Kojima M (2006b) The neuropeptide neuromedin U activates eosinophils and is involved in allergen-induced eosinophilia. *Am J Physiol Lung Cell Mol Physiol* **290**(5): L971-977.

Moriyama M, Matsukawa A, Kudoh S, Takahashi T, Sato T, Kano T, Yoshimura A and Kojima M (2006a) The neuropeptide neuromedin U promotes IL-6 production from macrophages and endotoxin shock. *Biochem Biophys Res Commun* **341**(4): 1149-1154.

Moriyama M, Sato T, Inoue H, Fukuyama S, Teranishi H, Kangawa K, Kano T, Yoshimura A and Kojima M (2005) The neuropeptide neuromedin U promotes inflammation by direct activation of mast cells. *J Exp Med* **202**(2): 217-224.

Nakahara K, Katayama T, Maruyama K, Ida T, Mori K, Miyazato M, Kangawa K and Murakami N (2010) Comparison of feeding suppression by the anorexigenic hormones neuromedin U and neuromedin S in rats. *J Endocrinol* **207**(2): 185-193.

Oakley RH, Laporte SA, Holt JA, Barak LS and Caron MG (1999) Association of beta-arrestin with G protein-coupled receptors during clathrin-mediated endocytosis dictates the profile of receptor resensitization. *J Biol Chem* **274**(45): 32248-32257.

Oakley RH, Laporte SA, Holt JA, Barak LS and Caron MG (2001) Molecular determinants underlying the formation of stable intracellular G protein-coupled receptor-beta-arrestin complexes after receptor endocytosis*. *J Biol Chem* **276**(22): 19452-19460.

Padilla BE, Cottrell GS, Roosterman D, Pikios S, Muller L, Steinhoff M and Bunnett NW (2007) Endothelin-converting enzyme-1 regulates endosomal sorting of calcitonin receptor-like receptor and beta-arrestins. *Journal of Cell Biology* **179**(5): 981-997.

Peier AM, Desai K, Hubert J, Du X, Yang L, Qian Y, Kosinski JR, Metzger JM, Pocai A, Nawrocki AR, Langdon RB and Marsh DJ (2011) Effects of Peripherally Administered Neuromedin U on Energy and Glucose Homeostasis. *Endocrinology*.

Pelayo JC, Poole DP, Steinhoff M, Cottrell GS and Bunnett NW (2011) Endothelin-converting enzyme-1 regulates trafficking and signalling of the neurokinin 1 receptor in endosomes of myenteric neurones. *J Physiol* **589**(Pt 21): 5213-5230.

Pierce KL, Premont RT and Lefkowitz RJ (2002) Seven-transmembrane receptors. *Nat Rev Mol Cell Biol* **3**(9): 639-650.

Pitcher JA, Freedman NJ and Lefkowitz RJ (1998) G protein-coupled receptor kinases. *Annu Rev Biochem* **67**: 653-692.

Poole DP and Bunnett NW (2016) G Protein-Coupled Receptor Trafficking and Signalling in the Enteric Nervous System: The Past, Present and Future. *Adv Exp Med Biol* **891**: 145-152.

Prendergast CE, Morton MF, Figueroa KW, Wu X and Shankley NP (2006) Species-dependent smooth muscle contraction to Neuromedin U and determination of the receptor subtypes mediating contraction using NMU1 receptor knockout mice. *Br J Pharmacol* **147**(8): 886-896.

Qi JS, Minor LK, Smith C, Hu B, Yang J, Andrade-Gordon P and Damiano B (2005) Characterization of functional urotensin II receptors in human skeletal muscle myoblasts: comparison with angiotensin II receptors. *Peptides* **26**(4): 683-690.

Raddatz R, Wilson AE, Artymyshyn R, Bonini JA, Borowsky B, Boteju LW, Zhou S, Kouranova EV, Nagorny R, Guevarra MS, Dai M, Lerman GS, Vaysse PJ, Branchek TA, Gerald C, Forray C and Adham N (2000) Identification and characterization of two neuromedin U receptors differentially expressed in peripheral tissues and the central nervous system. *J Biol Chem* **275**(42): 32452-32459.

Rani S, Corcoran C, Shiels L, Germano S, Breslin S, Madden S, McDermott MS, Browne BC, O'Donovan N, Crown J, Gogarty M, Byrne AT and O'Driscoll L (2014) Neuromedin U: a

candidate biomarker and therapeutic target to predict and overcome resistance to HER-tyrosine kinase inhibitors. *Cancer Res* **74**(14): 3821-3833.

Roosterman D, Cottrell GS, Padilla BE, Muller L, Eckman CB, Bunnett NW and Steinhoff M (2007) Endothelin-converting enzyme 1 degrades neuropeptides in endosomes to control receptor recycling. *Proceedings of the National Academy of Sciences of the United States of America* **104**(28): 11838-11843.

Roosterman D, Kempkes C, Cottrell GS, Padilla BE, Bunnett NW, Turck CW and Steinhoff M (2008) Endothelin-converting enzyme-1 degrades internalized somatostatin-14. *Endocrinology* **149**(5): 2200-2207.

Schmidlin F, Dery O, DeFea KO, Slice L, Patierno S, Sternini C, Grady EF and Bunnett NW (2001) Dynamin and Rab5a-dependent trafficking and signaling of the neurokinin 1 receptor. *Journal of Biological Chemistry* **276**(27): 25427-25437.

Shan L, Qiao X, Crona JH, Behan J, Wang S, Laz T, Bayne M, Gustafson EL, Monsma FJ, Jr. and Hedrick JA (2000) Identification of a novel neuromedin U receptor subtype expressed in the central nervous system. *J Biol Chem* **275**(50): 39482-39486.

Shenoy SK and Lefkowitz RJ (2011) beta-Arrestin-mediated receptor trafficking and signal transduction. *Trends Pharmacol Sci* **32**(9): 521-533.

Shetzline SE, Rallapalli R, Dowd KJ, Zou S, Nakata Y, Swider CR, Kalota A, Choi JK and Gewirtz AM (2004) Neuromedin U: a Myb-regulated autocrine growth factor for human myeloid leukemias. *Blood* **104**(6): 1833-1840.

Stott LA, Hall DA and Holliday ND (2016) Unravelling intrinsic efficacy and ligand bias at G protein coupled receptors: A practical guide to assessing functional data. *Biochemical pharmacology* **101**: 1-12.

Szekeres PG, Muir AI, Spinage LD, Miller JE, Butler SI, Smith A, Rennie GI, Murdock PR, Fitzgerald LR, Wu H, McMillan LJ, Guerrera S, Vawter L, Elshourbagy NA, Mooney JL, Bergsma DJ, Wilson S and Chambers JK (2000) Neuromedin U is a potent agonist at the orphan G protein-coupled receptor FM3. *J Biol Chem* **275**(27): 20247-20250.

Thompson GL, Lane JR, Coudrat T, Sexton PM, Christopoulos A and Canals M (2015) Biased Agonism of Endogenous Opioid Peptides at the mu-Opioid Receptor. *Mol Pharmacol* **88**(2): 335-346.

Thomsen AR, Plouffe B, Cahill TJ, 3rd, Shukla AK, Tarrasch JT, Dosey AM, Kahsai AW, Strachan RT, Pani B, Mahoney JP, Huang L, Breton B, Heydenreich FM, Sunahara RK, Skiniotis G, Bouvier M and Lefkowitz RJ (2016) GPCR-G Protein-beta-Arrestin Super-Complex Mediates Sustained G Protein Signaling. *Cell* **166**(4): 907-919.

Umekawa K, Hasegawa H, Tsutsumi Y, Sato K, Matsumura Y and Ohashi N (2000) Pharmacological characterization of a novel sulfonylureid-pyrazole derivative, SM-19712, a potent nonpeptidic inhibitor of endothelin converting enzyme. *Jpn J Pharmacol* **84**(1): 7-15.

Yamasaki-Mann M, Demuro A and Parker I (2009) cADPR stimulates SERCA activity in Xenopus oocytes. *Cell calcium* **45**(3): 293-299.

Yarwood RE, Imlach WL, Lieu T, Veldhuis NA, Jensen DD, Klein Herenbrink C, Aurelio L, Cai Z, Christie MJ, Poole DP, Porter CJH, McLean P, Hicks GA, Geppetti P, Halls ML, Canals M and Bunnett NW (2017) Endosomal signaling of the receptor for calcitonin gene-related peptide mediates pain transmission. *Proc Natl Acad Sci U S A*.

Molecular Pharmacology Fast Forward. Published on May 3, 2018 as DOI: 10.1124/mol.117.111070
This article has not been copyedited and formatted. The final version may differ from this version.

Footnotes

The authors would like to gratefully acknowledge funding from King Saud University, Riyadh, Kingdom of Saudi Arabia (KA), Tabuk University, Kingdom of Saudi Arabia (OB) and The Higher Committee for Education Development in Iraq and University of Kufa, School of Medicine, Iraq (HQ).

Molecular Pharmacology Fast Forward. Published on May 3, 2018 as DOI: 10.1124/mol.117.111070
This article has not been copyedited and formatted. The final version may differ from this version.

Figure legends

Fig. 1. Ca^{2+} responses in HEK-NMU2 to applications of either hNmU-25 or carbachol. Cells were loaded with fluo-4-AM and changes in cytosolic fluorescence intensity measured as an index of $[Ca^{2+}]_i$ using confocal microscopy. Cells were challenged with either (**A**) hNmU-25 (30 nM) or (**B**) carbachol (Cch, 300 μM) at t=30 s for 60 s. Cells were then perfused with KHB and after 5 min, the same ligand was re-applied to the cells. Changes in fluo-4 fluorescence are shown relative to the basal level. The dashed lines indicate where data were not collected. Each line represents data from a single cell and each representative image (a-d) was taken at the points indicated on the time-course graph. Data are representative of 3 separate experiments, with at least 5 cells observed in each experiment.

Fig. 2. Visualizing ligand binding and the removal of ligand bound to NMU2. HEK-NMU2 cells were challenged with the fluorescently-labeled NmU ligand, Cy3B-pNmU-8 (10 nM) and visualized by confocal microscopy. Panel (**Ai**) shows fluorescence directly after addition of Cy3B-pNmU-8. Cells were then washed with KHB (5 mL/min) pH 7.4 (**Aii**) followed by a brief, 30 s wash with KHB at pH 4 (**Aiii**), pH 3.5 (**Aiv**), pH 3.0 (**Av**), or pH 2.0 (**Avi**). Panel (**Bi**) shows fluorescence 60 s after addition of Cy3B-pNmU-8 (10 nM) and immediately following a brief (≤25 s) wash with KHB at pH 2.0 (**Bii**). Further images were taken after perfusion with KHB, pH 7.4 (5 mL/min) for 5 min (**Biii**) or following re-application of Cy3B-pNmU-8 (**Biv**). Temperature was maintained at 12ºC to prevent receptor internalization. Images are representative of at least 3 experiments where similar results were obtained.

Fig. 3. Ca^{2+} responses in HEK293-NMU2 are unaltered by brief acid washing. For a 5 min recovery period (**A**) HEK-NMU2cells were loaded with fluo-4-AM and then exposed to a brief wash (≤25 s) with KHB at either pH 7.4 or pH 2.0 followed by three washes with KHB (pH 7.4). Cells were then challenged with hNmU-25 and changes in fluorescence intensity measured as an index of $[Ca^{2+}]_i$. For the 2 h recovery period (**B**), cells were washed as above, but loaded with fluo-4-AM during the last 45 min of the 2 h recovery period. For either recovery period, maximal changes in fluorescence following hNmU-25 challenge were determined and used to construct concentration-responses curves. Data are means ± s.e.m., n=3. For imaging experiments fluo-4-AM-loaded cells were challenged with either (**C**) hNmU-25 (30 nM) or (**D**) carbachol (Cch, 300 μM) at t=30 s for 60 s. Cells were then

perfused briefly (≤20 s) with KHB pH 2.0 followed by perfusion with KHB pH 7.4 and after approximately 6 min, the same ligand was used to re-challenge the cells. The dashed lines indicate periods when data were not collected. Each line represents data from a single cell and each representative image (a-d) was taken at the points indicated on the time-course graph. Data are representative of 3 separate experiments, with at least 5 cells observed in each experiment.

Fig. 4. Effect of the duration of pre-exposure to hNmU-25 on homologous desensitization of NMU2. HEK-NMU2 were loaded with fluo-4-AM and challenged with either buffer, or hNmU-25 (30 nM) for 1, 3, 5 or 30 min. Following the initial agonist challenge, cells were briefly (≤25 s) washed with acidified KHB, pH 2.0 and washed twice with KHB, pH 7.4 and left in the latter buffer for 5 min. Cells were then stimulated with hNmU-25 (30 nM) and changes in fluorescence intensity measured as an index of $[Ca^{2+}]_i$ using a NOVOstar plate-reader. **A**) Experimental protocol. **B**) Representative Ca^{2+} responses to hNmU-25 (30 nM) in HEK-NMU2 pre-exposed to buffer only (control) for 5 min or hNmU-25 (30 nM) for 1, 3, 5 or 30 min. **C**) Maximal changes in cytosolic fluorescence following the second hNmU-25 challenge. Data are means ± s.e.m., n=3; $^{**}P<0.01$, $^{***}P<0.001$ by Bonferroni's multiple comparison test following one-way ANOVA.

Fig. 5. Resensitization of Ca^{2+} responses to hNmU-25 in HEK-NMU2 following ligand removal using the standard or brief acid-wash protocol. For experiments in which a 5 min recovery period following an initial agonist challenge was required, cells were loaded with fluo-4-AM and then challenged with either buffer (control) or hNmU-25 (30 nM) for 5 min. For the longer (1-6 h) recovery periods, cells were challenged and washed as above, but loaded with fluo-4-AM during the last 45 min of the recovery period. Initial agonist exposure was followed by a brief wash (≤25 s) with either (**A**) standard KHB, pH 7.4 or (**B**) acidified KHB, pH 2.0 followed by two washes and a 5 min recovery period in KHB, pH 7.4. Cells were subsequently re-challenged with different concentrations of hNmU-25 (0.1-100 nM) and fluorescence monitored using a NOVOstar plate-reader. Concentration-response curves were constructed based on maximal changes in fluorescence as an index of $[Ca^{2+}]_i$ and expressed as a percentage of the maximum response in HEK-NMU2 pre-exposed to buffer only (i.e. no initial hNmU-25 challenge). Control concentration-response curves were generated for each

time-point and were not significantly different from each other. Data are mean ± s.e.m., n=3-6.

Fig. 6. Comparison of NMU2 desensitization and resensitization following challenge with hNmU-25 or hNmS-33. Fluo-4-loaded cells were either untreated ('0'), or pre-treated with hNmU-25 (30 nM**, A**) or hNmS-33 (30 nM, **B**), and then washed with KHB, pH 7.4. After a further 1-10 min recovery, cells were re-challenged with 30 nM of the same ligand and Ca^{2+} responses determined. Alternatively, cells were untreated or pre-treated with either 30 nM hNmU-25 or hNmS-33 for 5 min, then washed and left to recover for 1, 3 or 6 h. During the final 45 min of the recovery period, cells were loaded with fluo-4-AM and then re-challenged with 30 nM ligand using a NOVOstar plate-reader to allow determination of the Ca^{2+} responses (**C**). Data are means ± s.e.m., n=3; $^{*}P<0.05$, $^{**}P<0.01$, $^{***}P<0.001$ by Bonferroni's multiple comparison test following one-way ANOVA (panels A, B), or unpaired Student's t-test (panel C).

Fig. 7. Co-internalization of ligand and NMU2. HEK-293 stably expressing the NMU2 with a *C*-terminal EGFP tag (NMU2-EGFP) were cultured on 25 mm glass coverslips for 24-48 h. Cells were challenged with Cy3B-pNmU-8 (10 nM, **A**) in KHB and visualized immediately (0 min) or after 25 min (at 37^{o}C) by confocal microscopy consecutively at 488 nm and 568 nm to image NMU2-EGFPand Cy3B-pNmU-8. NMU2-EGFP and Cy3B-pNmU-8 images were merged (**A**, right panels) post-acquisition. Data are representative of 3 independent experiments where similar results were obtained. NMU2-EGFP was also visualized by confocal microscopy during challenge with 30 nM of either hNmU-25 (**Ba-d**) or hNmS-33 (**Be-h**). NMU2-EGFP internalization was then calculated as described in *Methods* and plotted as a function of time (**C**). Data are means ± s.e.m., n=4-5 cells.

Fig. 8. Effects of inhibitors of receptor internalization, endosomal acidification or protein synthesis on NMU2 resensitization following challenge with either hNmU-25 or hNmS-33. HEK-NMU2 were pre-incubated in the absence or presence of an inhibitor of receptor internalization (dynasore, 80 μM, **A**, **B**), endosomal acidification (monensin, 50 μM, **C**, **D**), or protein synthesis (cycloheximide, 17.5 μM, **E**, **F**) for 30 min before challenge with buffer or ligands (hNmU-25 (**A**, **C**, **E**) or hNmS-33 (**B**, **D**, **F**), each at 30 nM for 5 min). Cells were washed and allowed to recover for 6 h (± inhibitor) before determination of the Ca^{2+} response

Molecular Pharmacology Fast Forward. Published on May 3, 2018 as DOI: 10.1124/mol.117.111070
This article has not been copyedited and formatted. The final version may differ from this version.

to the same ligand (30 nM). Data show maximal responses following addition of ligand and are means ± s.e.m., n=3; $^{*}P<0.05$, $^{**}P<0.01$, $^{***}P<0.001$ by Bonferroni's multiple comparison test following one-way ANOVA.

Fig. 9. Effect of the ECE-1 inhibitor, SM-19712, on NMU2 resensitization. For the 5 min recovery protocol cells were pre-incubated in the absence or presence of SM-19712 (10 µM, 30 min) and loaded with fluo-4-AM before challenge with hNmU-25 (30 nM, **A**), hNmS-33 (30 nM, **B**), carbachol (100 µM, **C**) or buffer for 5 min followed by two KHB washes and a 5 min recovery period in KHB. For longer recovery periods (1-6 h), cells were pre-treated with SM-19712 (10 µM, 30 min) or vehicle and then challenged with ligand or buffer and washed as above: during the last 45 min of the recovery period, cells were loaded with fluo-4-AM. Following the recovery period, cells were challenged with hNmU-25 (30 nM, **A**), hNmS-33 (30 nM, **B**), or carbachol (100 µM, **C**) and changes in cytosolic fluorescence recorded using a NOVOstar plate-reader as an index of changes in $[Ca^{2+}]_i$. Data are expressed as a percentage of the maximum response to ligand in HEK-NMU2 challenged initially with buffer only. Alternatively, cells were challenged with buffer or hNmU-25 (30 nM, 5 min), washed and allowed to recover for 3 h in the presence or absence of SM-19712 (10 µM) that was only added after ligand stimulation and washing (**D**). Data are means ± s.e.m., n=3-6 in duplicate; $^{***}P<0.001$ by Bonferroni's multiple comparison test following two-way ANOVA (panel A) and one-way ANOVA (panel D).

Fig. 10. Cellular depletion of ECE-1 impairs resensitization following hNmU-25, but not hNmS-33 challenge. Cells were transfected with either anti-ECE-1 siRNA or a scrambled siRNA and the expression of ECE-1 determined 48 h later by immunoblotting. Total ERK1/2 immunoreactivity was used as a loading control (**A**). Cells transfected with either anti-ECE-1 siRNA (+) or scrambled siRNA (-) for 48 h were pre-treated with buffer, hNmU-25 (**B**) or hNmS-33 (**C**) (both at 30 nM for 5 min) and then washed with KHB. Cells were allowed to recover for 6 h, loaded with fluo-4-AM during the final 45 min and then challenged or re-challenged with the same concentration of each respective ligand. Changes in cytosolic fluorescence were recorded using a NOVOstar plate-reader as an index of $[Ca^{2+}]_i$. Data are representative or means ± s.e.m., n=3 and were analyzed by Student's paired *t* test (panel A), or Bonferroni's multiple comparison test following one-way ANOVA (panels B, C); $^{*}P<0.05$, $^{**}P<0.01$, $^{***}P<0.001$.

Molecular Pharmacology Fast Forward. Published on May 3, 2018 as DOI: 10.1124/mol.117.111070
This article has not been copyedited and formatted. The final version may differ from this version.

Fig. 11. Time-course of NMU2-mediated activation of ERK1/2 in the presence and absence of ECE-1 inhibition in the continued presence of ligand. HEK-NMU2 were incubated with or without SM-19712 (10 μM) for 30 min prior to challenge with hNmU-25 (30 nM) (**A**), or hNmS-33 (30 nM) (**B**). Cells were then left for the required time before solubilization and assessment of pERK by immunoblotting and densitometry. Data are representative or means ± s.e.m. of n=3. Ribosomal S6 protein (Total S6) is shown as a loading control. Note that pERK and total S6 were identified on the same blot but are shown here with different exposure times for clarity.

Fig. 12. Time-course of NMU2-mediated activation of ERK1/2 and p38 MAPK in the presence and absence of ECE-1 inhibition following removal of free, extracellular ligand. HEK-NMU2 were incubated with or without SM-19712 (10 μM) for 30 min prior to challenge with hNmU-25 (30 nM) (**A**, **C**), or hNmS-33 (30 nM) (**B**, **D**) for 5 min. Free, extracellular ligand was then removed by washing the monolayer twice with KHB and the cells then left in KHB for the required time before assessment of either pERK (**A**, **B**) or pp38 (**C**, **D**) immunoreactivity. Data are representative or means ± s.e.m. of n=3. '0' represents the point immediately before ligand addition; 5* represents the point of ligand removal; other times represent the points following ligand removal. $^{**}P<0.01$, $^{***}P<0.001$ by Bonferroni's multiple range test following two-way ANOVA. Levels of ribosomal S6 protein were assessed (see Figure 11) to ensure equivalent loading but are not shown here for clarity.

Molecular Pharmacology Fast Forward. Published on May 3, 2018 as DOI: 10.1124/mol.117.111070
This article has not been copyedited and formatted. The final version may differ from this version.

TABLE 1

Resensitization of Ca^{2+} responses to hNmU-25 in HEK-NMU2 following ligand washout using the standard or brief acid-wash protocol

Data are derived from the concentration-response curves shown in Figure 5, demonstrating changes in pEC_{50} and E_{max} values during recovery from hNmU-25-mediated desensitization. For full details see legend to Figure 5 and *Methods*. Data are means ± s.e.m., n=3-6. $^{*}P<0.05$ and $^{***}P<0.001$ versus control by Bonferroni's multiple comparison test following one-way ANOVA. NA, not applicable.

Recovery time	KHB wash (pH 7.4)		Acidified buffer wash (pH 2.0)	
	pEC_{50}	E_{max} (%)	pEC_{50}	E_{max} (%)
Control	9.29 ± 0.06	100	9.26 ± 0.06	100
5 min	NA	3.1 ± 1.1	8.51 ± 0.07*	32.7 ± 4.2
1 h	NA	9.4 ± 1.7	8.89 ± 0.38	81.4 ± 6.4
2 h	8.62 ± 0.29*	29.1 ± 5.9	9.22 ± 0.03	89.4 ± 4.1
3 h	8.24 ± 0.23***	56.4 ± 4.7	-	-
6 h	9.07 ± 0.07	96.0 ± 4.0	-	-

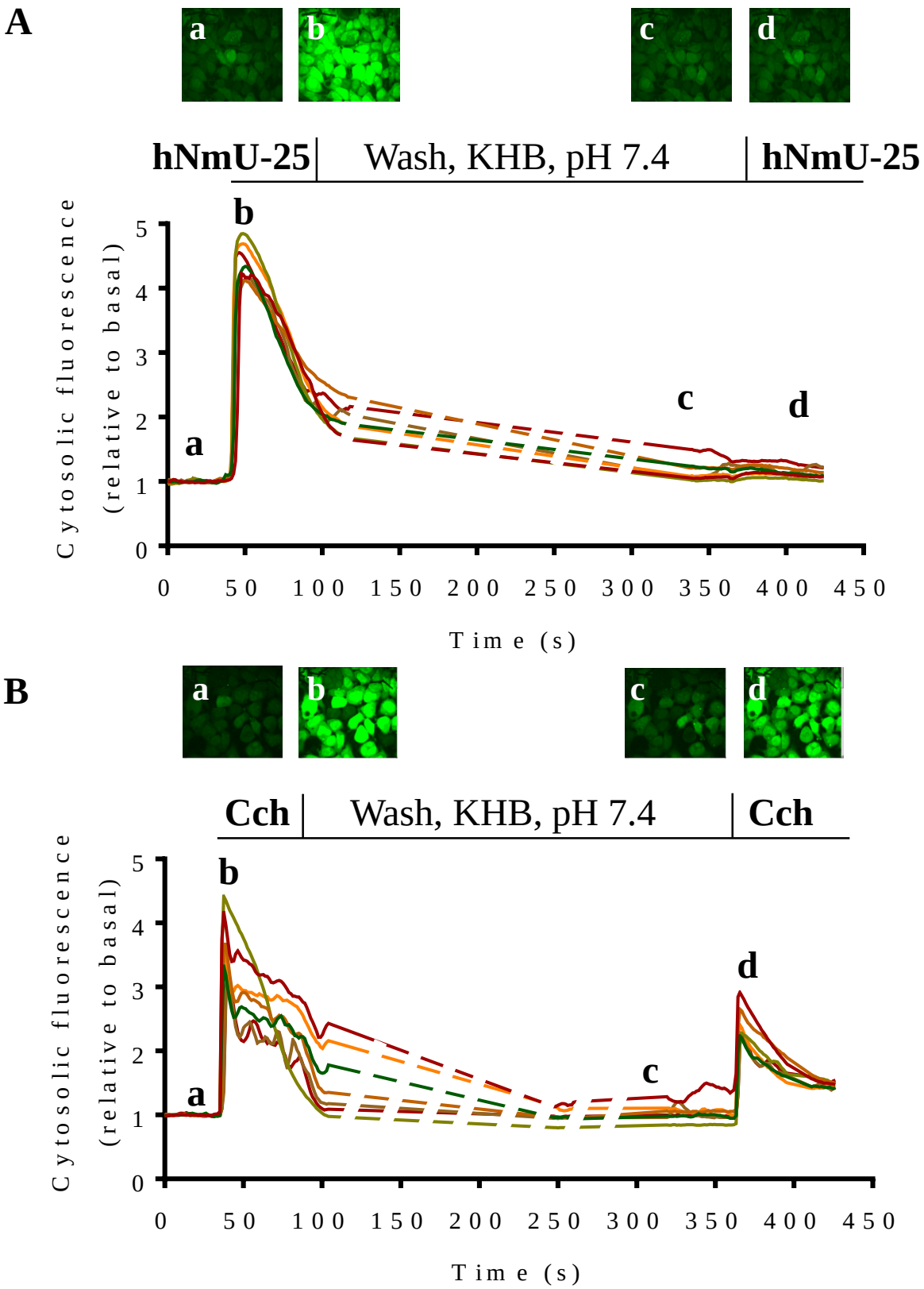
A
a
b
c
d
hNmU-25
Wash, KHB, pH 7.4
hNmU-25
Cytosolic fluorescence
(relative to basal)
0
1
2
3
4
5
0
50
100
150
200
250
300
350
400
450
Time (s)
B
a
b
c
d
Cch
Wash, KHB, pH 7.4
Cch
Cytosolic fluorescence
(relative to basal)
0
1
2
3
4
5
0
50
100
150
200
250
300
350
400
450
Time (s)

Figure 1

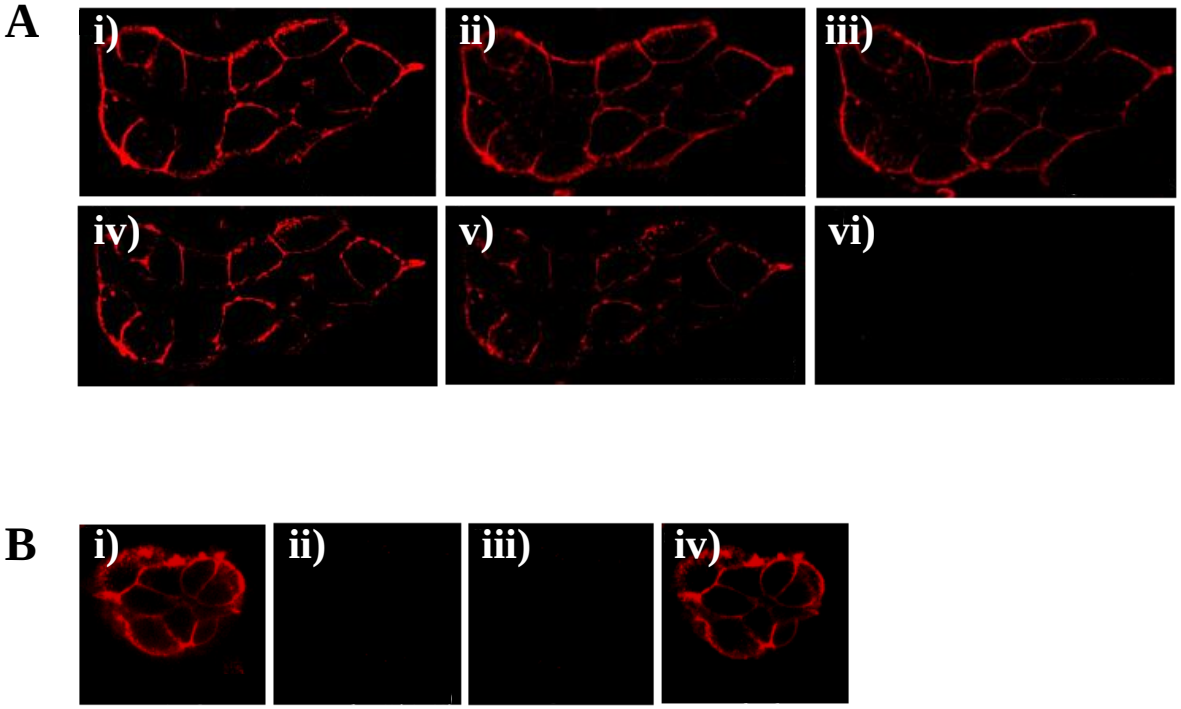

Figure 2

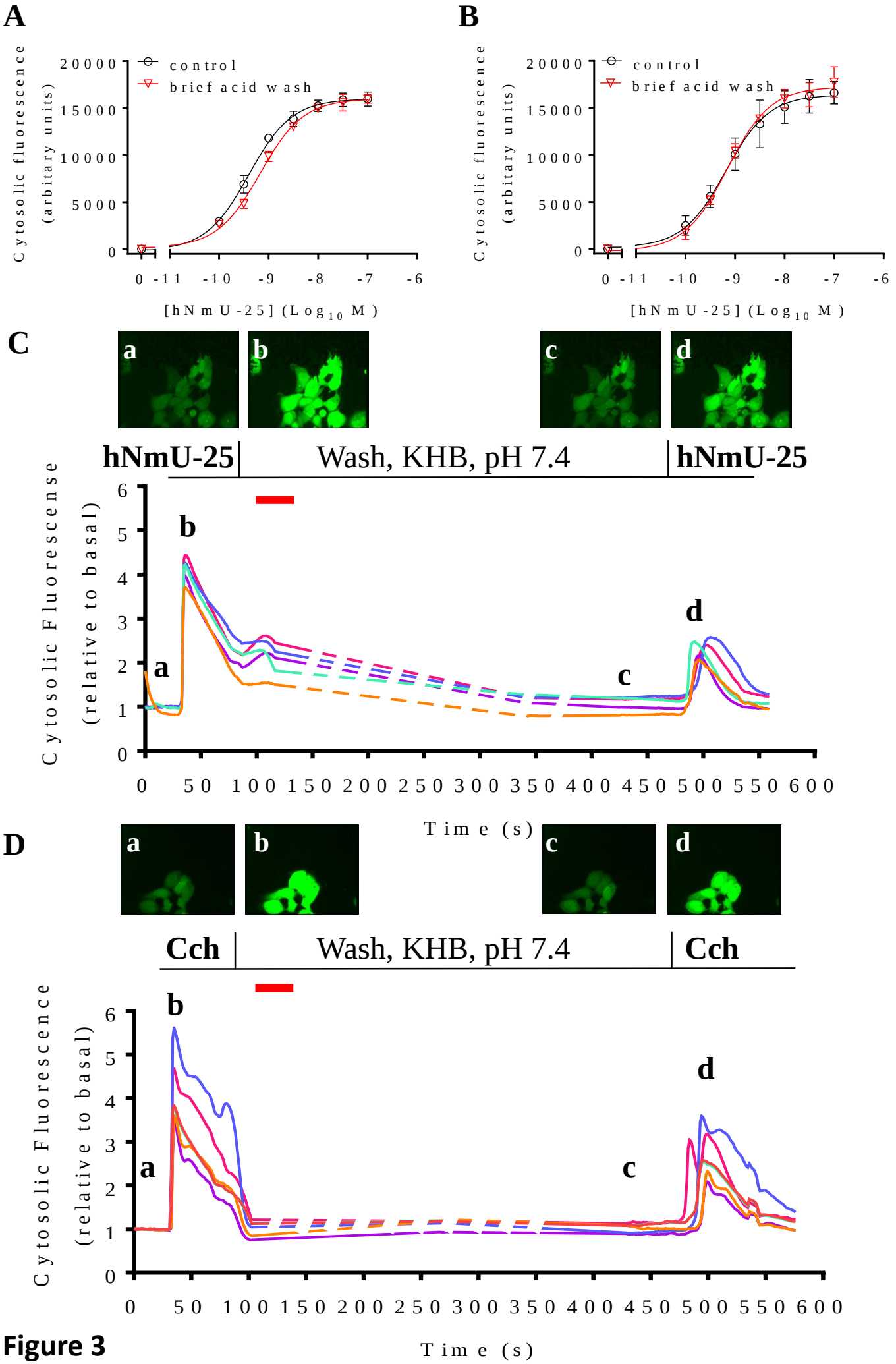
A
B
C
D
control
brief acid wash
Cytosolic fluorescence (arbitary units)
[hNmU-25] (Log10 M)
a
b
c
d
hNmU-25
Wash, KHB, pH 7.4
hNmU-25
Cytosolic Fluorescense (relative to basal)
Time (s)
Cch
Wash, KHB, pH 7.4
Cch
Cytosolic Fluorescence (relative to basal)
Time (s)

Figure 3

A

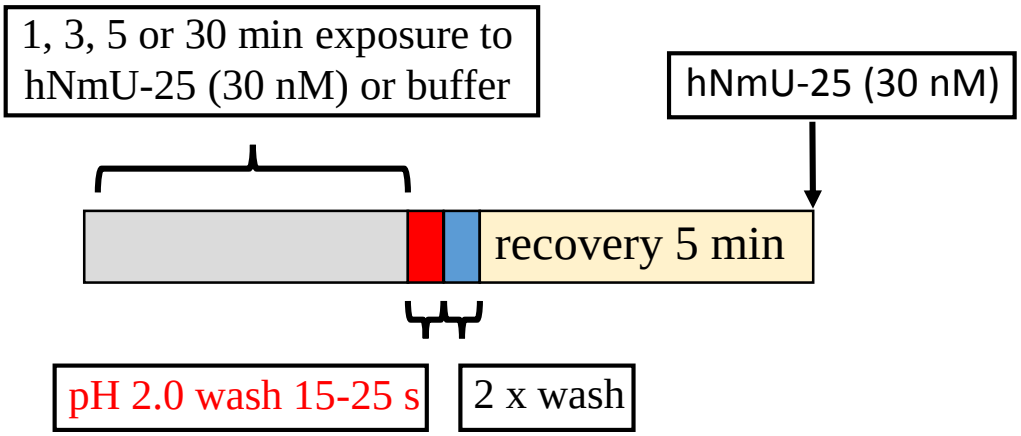
1, 3, 5 or 30 min exposure to hNmU-25 (30 nM) or buffer
hNmU-25 (30 nM)
recovery 5 min
pH 2.0 wash 15-25 s
2 x wash

B

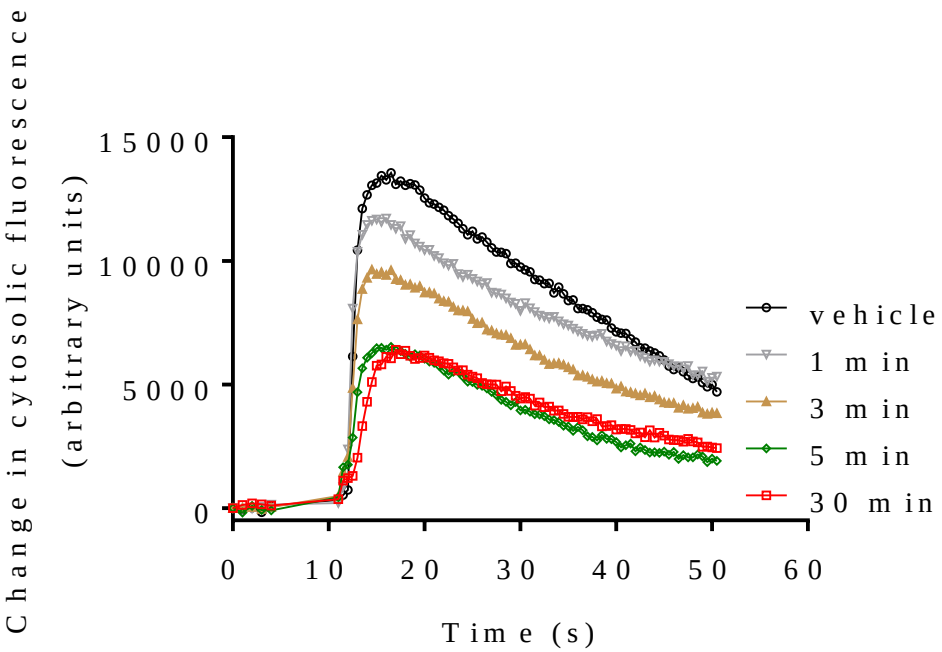
Change in cytosolic fluorescence (arbitrary units)
15000
10000
5000
0
0
10
20
30
40
50
60
Time (s)
vehicle
1 min
3 min
5 min
30 min

C

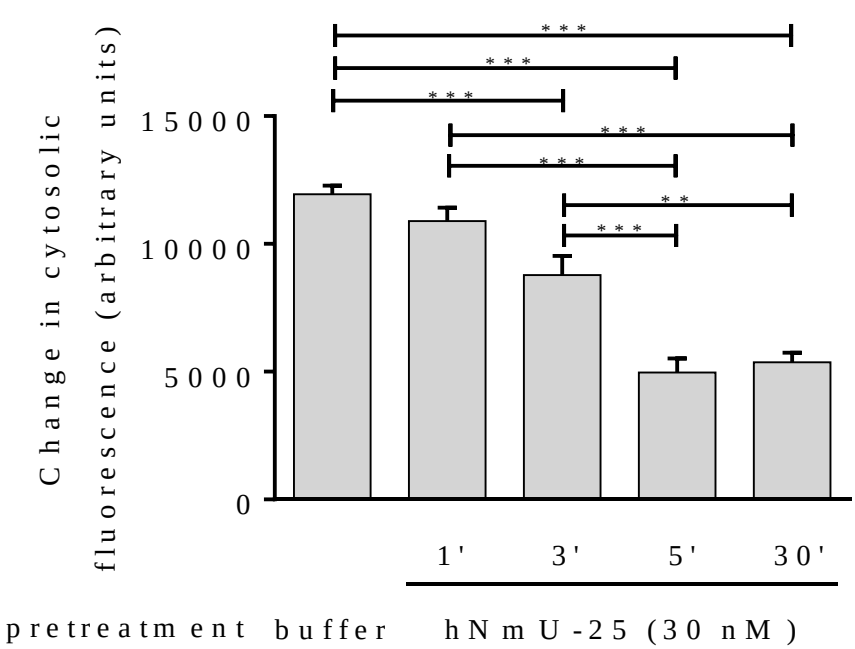
Change in cytosolic fluorescence (arbitrary units)
15000
10000
5000
0
***
***
***
***
***
**
***
1'
3'
5'
30'
pretreatment buffer
hNmU-25 (30 nM)

Figure 4

A

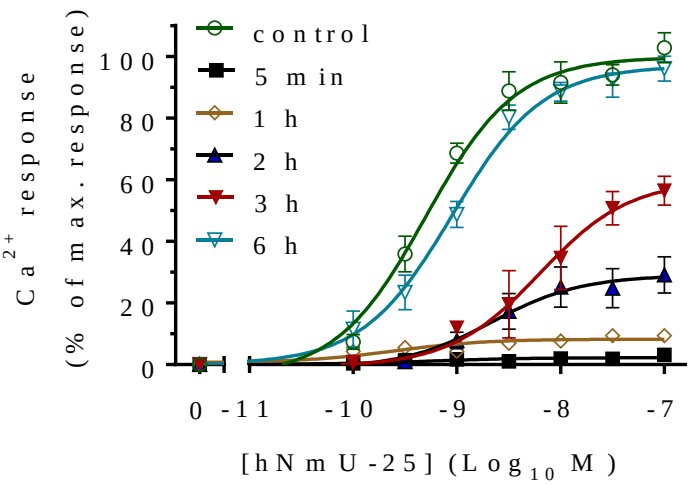
control
5 min
1 h
2 h
3 h
6 h
Ca2+ response
(% of max. response)
100
80
60
40
20
0
0 -11 -10 -9 -8 -7
[hNmU-25] (Log10 M)

B

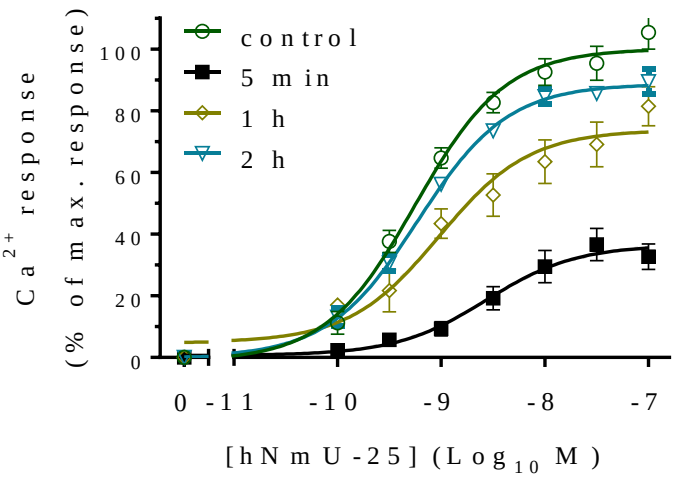
control
5 min
1 h
2 h
Ca2+ response
(% of max. response)
100
80
60
40
20
0
0 -11 -10 -9 -8 -7
[hNmU-25] (Log10 M)

Figure 5

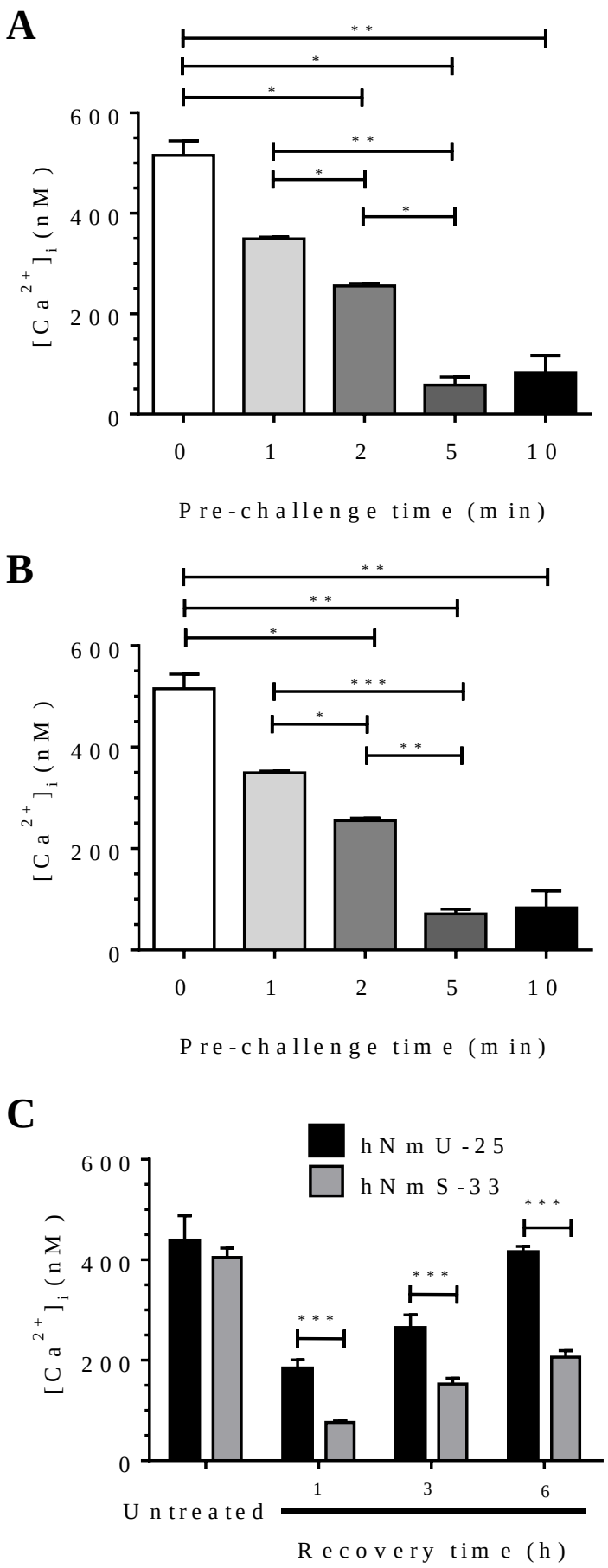
A
**
*
*
600
400
200
0
[Ca2+]i (nM)
**
*
*
0
1
2
5
10
Pre-challenge time (min)
B
**
**
*
600
400
200
0
[Ca2+]i (nM)
***
*
**
0
1
2
5
10
Pre-challenge time (min)
C
hNmU-25
hNmS-33
600
400
200
0
[Ca2+]i (nM)
***
***
***
1
3
6
Untreated
Recovery time (h)

Figure 6

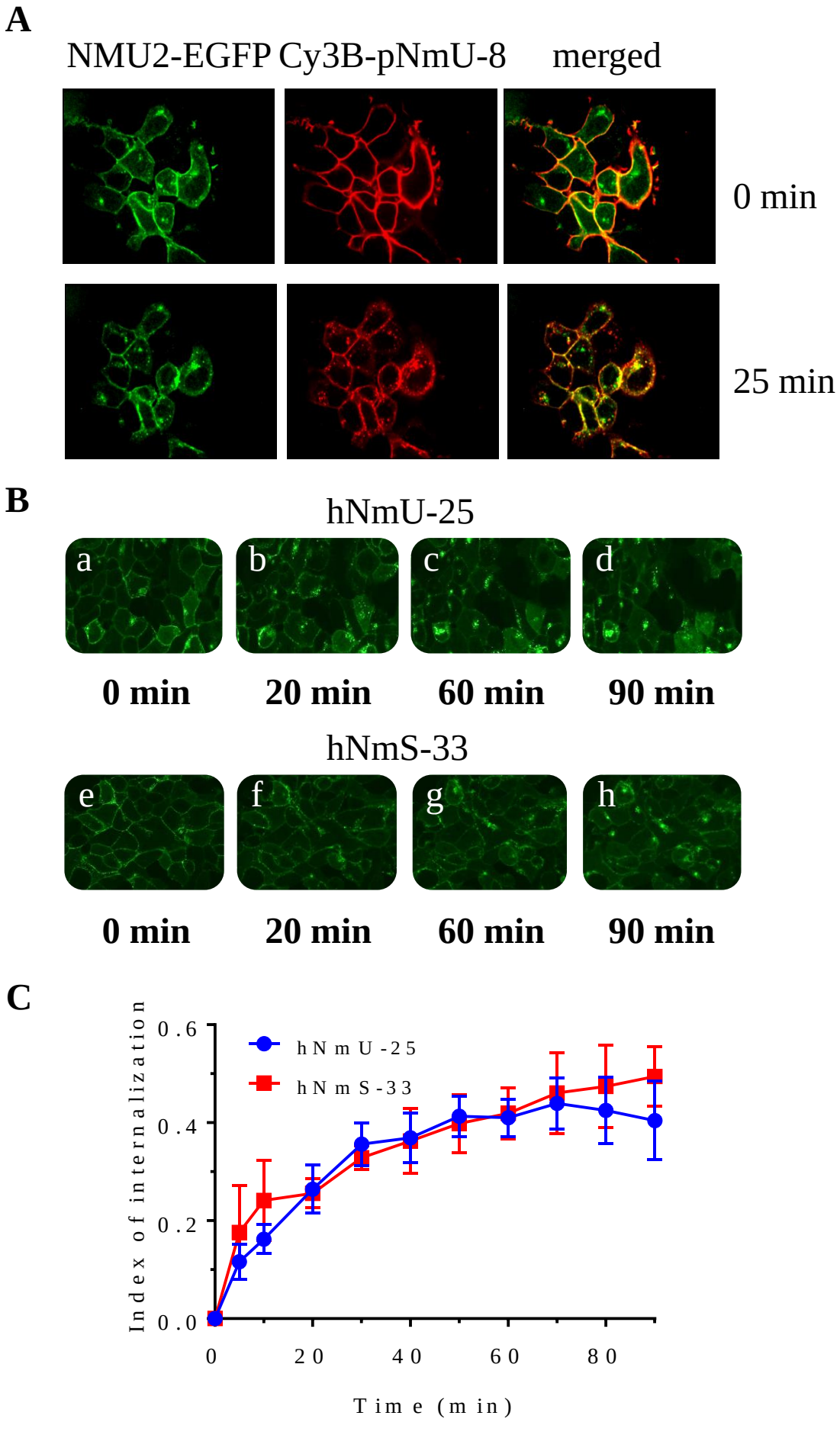
A
NMU2-EGFP
Cy3B-pNmU-8
merged
0 min
25 min
B
hNmU-25
a
b
c
d
0 min
20 min
60 min
90 min
hNmS-33
e
f
g
h
0 min
20 min
60 min
90 min
C
Index of internalization
0.0
0.2
0.4
0.6
hNmU-25
hNmS-33
0
20
40
60
80
Time (min)

Figure 7

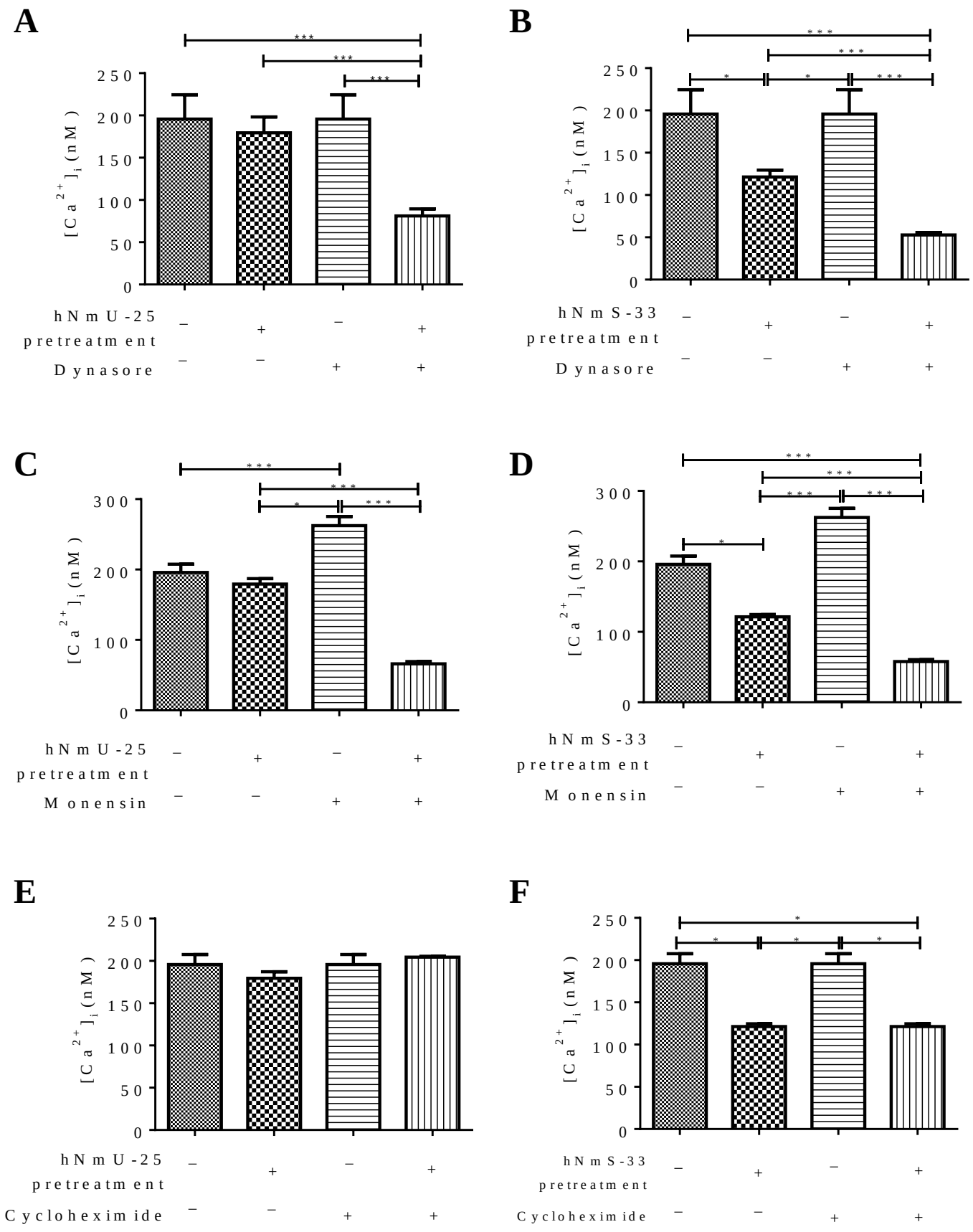
A
B
C
D
E
F
[Ca2+]i (nM)
hNmU-25 pretreatment
hNmS-33 pretreatment
Dynasore
Monensin
Cycloheximide
***
*

Figure 8

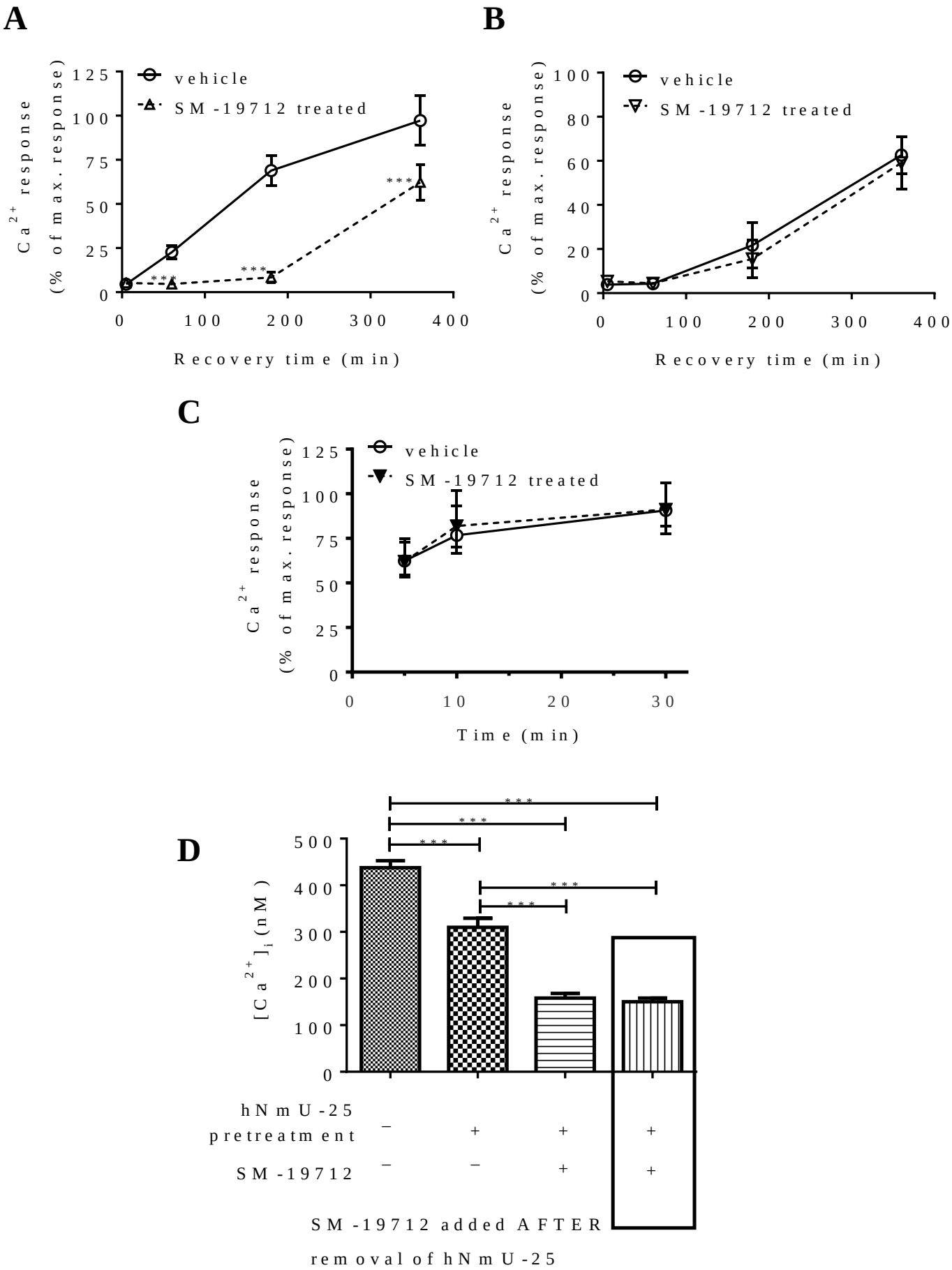
A
B
C
D
vehicle
SM-19712 treated
Ca2+ response (% of max. response)
Recovery time (min)
Time (min)
[Ca2+]i (nM)
hNmU-25 pretreatment
SM-19712
SM-19712 added AFTER removal of hNmU-25
***

Figure 9

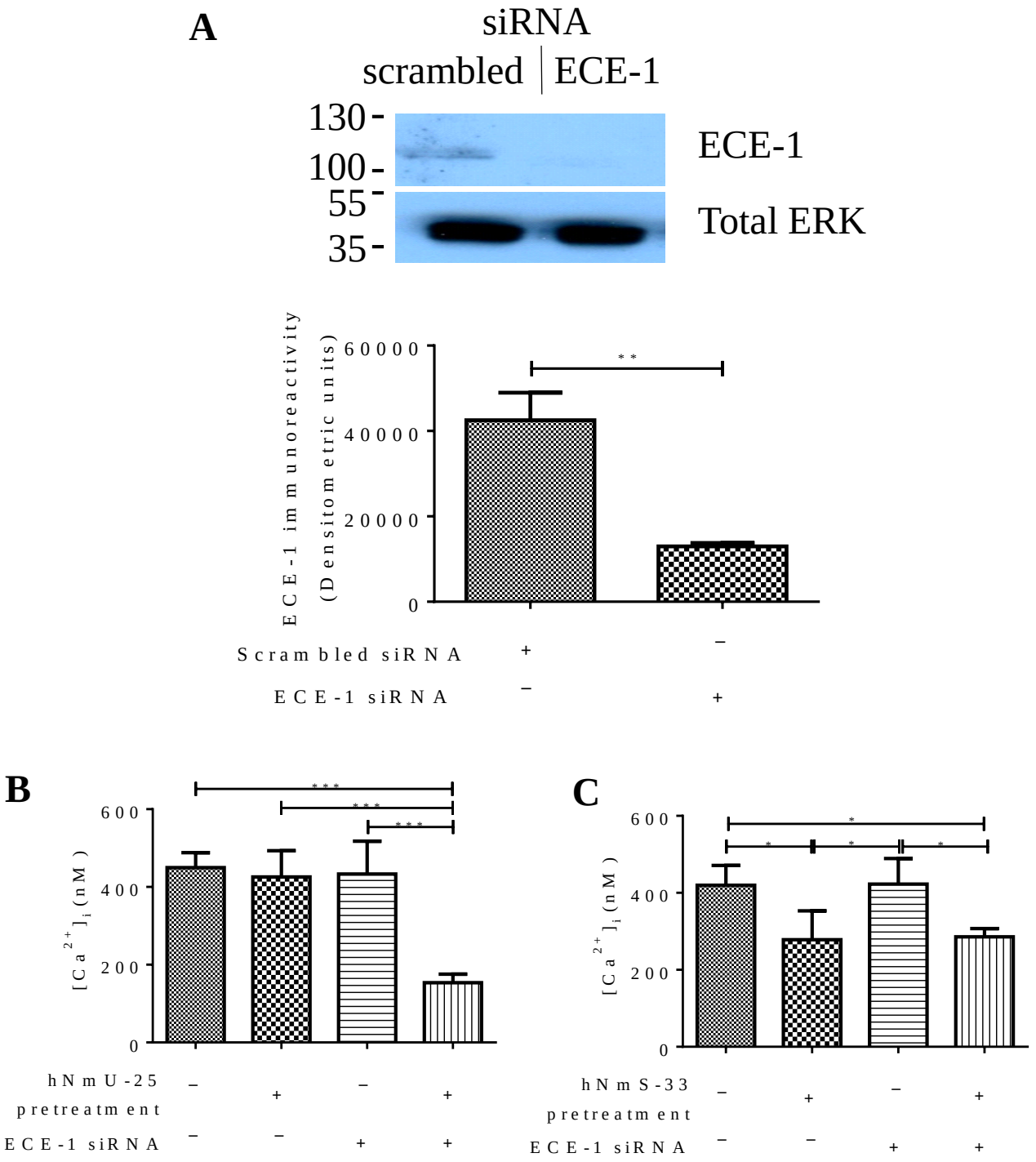
A
siRNA
scrambled
ECE-1
130
100
55
35
ECE-1
Total ERK
ECE-1 immunoreactivity (Densitometric units)
60000
40000
20000
0
**
Scrambled siRNA
ECE-1 siRNA
B
[Ca2+]i (nM)
600
400
200
0
***
***
***
hNmU-25 pretreatment
ECE-1 siRNA
C
[Ca2+]i (nM)
600
400
200
0
*
*
*
*
hNmS-33 pretreatment
ECE-1 siRNA

Figure 10

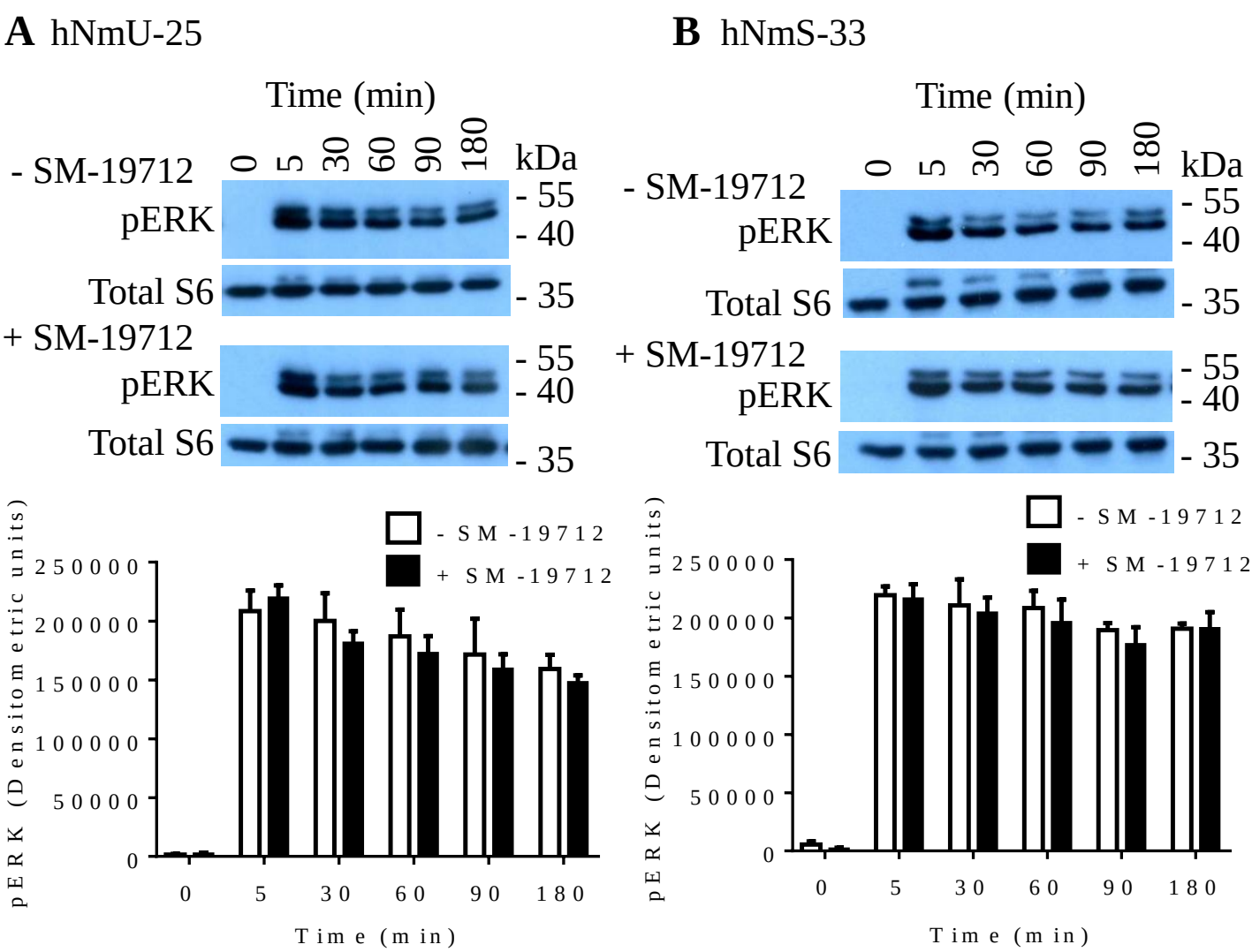
A hNmU-25
Time (min)
0 5 30 60 90 180
kDa
- SM-19712
pERK
- 55
- 40
Total S6
- 35
+ SM-19712
pERK
- 55
- 40
Total S6
- 35
- SM-19712
+ SM-19712
pERK (Densitometric units)
250000
200000
150000
100000
50000
0
0 5 30 60 90 180
Time (min)
B hNmS-33
Time (min)
0 5 30 60 90 180
kDa
- SM-19712
pERK
- 55
- 40
Total S6
- 35
+ SM-19712
pERK
- 55
- 40
Total S6
- 35
- SM-19712
+ SM-19712
pERK (Densitometric units)
250000
200000
150000
100000
50000
0
0 5 30 60 90 180
Time (min)

Figure 11

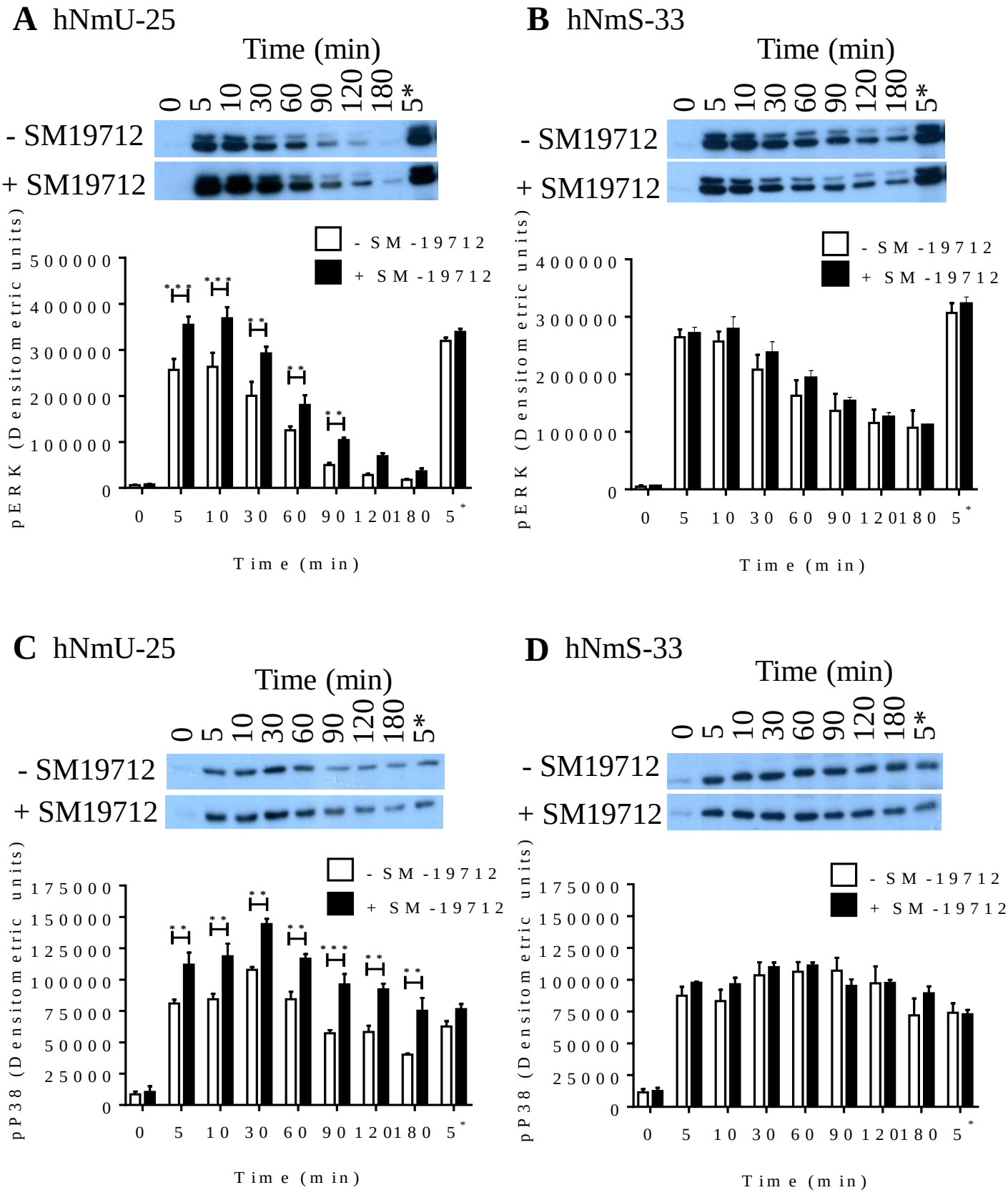
A hNmU-25
Time (min)
0 5 10 30 60 90 120 180 5*
- SM19712
+ SM19712
- SM -19712
+ SM -19712
pERK (Densitometric units)
500000
400000
300000
200000
100000
0
0 5 10 30 60 90 120 180 5*
Time (min)
B hNmS-33
Time (min)
0 5 10 30 60 90 120 180 5*
- SM19712
+ SM19712
- SM -19712
+ SM -19712
pERK (Densitometric units)
400000
300000
200000
100000
0
0 5 10 30 60 90 120 180 5*
Time (min)
C hNmU-25
Time (min)
0 5 10 30 60 90 120 180 5*
- SM19712
+ SM19712
- SM -19712
+ SM -19712
pP38 (Densitometric units)
175000
150000
125000
100000
75000
50000
25000
0
0 5 10 30 60 90 120 180 5*
Time (min)
D hNmS-33
Time (min)
0 5 10 30 60 90 120 180 5*
- SM19712
+ SM19712
- SM -19712
+ SM -19712
pP38 (Densitometric units)
175000
150000
125000
100000
75000
50000
25000
0
0 5 10 30 60 90 120 180 5*
Time (min)

Figure 12